MASTER THESIS

ENERGY TECHNOLOGY FOR SUSTAINABLE DEVELOPMENT

EXPERIMENTAL ANALYSIS OF THE REFRIGERANT FLOW MALDISTRIBUTION IN A BRAZED PLATE HEAT EXCHANGER

AUTHOR: **ÁLVAREZ PIÑEIRO, LUCAS**

TUTOR: NAVARRO PERIS, EMILIO

COTUTOR: CORBERÁN SALVADOR, JOSÉ MIGUEL

Academic Year: 2018-19

"September 2019"

ACKNOWLEDGEMENTS

Nestas líneas aproveito en primeiro lugar para darlle as gracias a Emilio Navarro, por todo o que me ensinou, aconsellou e corrixiu para ser un enxeñeiro de verdade…aínda que a el non lle gustan.

A José Miguel Corberán por darme a oportunidade de formar parte do IIE e deixarme ser un investigador.

Os compañeiros do IIE son o mellorciño que hai. Gracias por acollerme e por facerme un máis do equipo; marcho que teño que marchar!

Meus país que tanto me botan de menos. Gracias por ser os meus mellores fans.

Indudablemente tamén, a ti…

RESUMEN

Los intercambiadores de calor de placas soldadas se usan ampliamente en muchas aplicaciones industriales debido a su alta eficiencia, compacidad y rentabilidad. Para aplicaciones de recuperación de calor en bombas de calor, por ejemplo, la diferencia de temperatura en el fluido secundario puede ser superior a los utilizados en otras aplicaciones (alrededor de 5 K). Con la finalidad de encontrar la mejor estrategia para extraer la máxima cantidad de energía de aguas residuales con el mejor rendimiento global, el proyecto europeo "Next Generation of Heat Pumps working with Natural fluids" (NXTHPG) centra toda su atención en construir un prototipo de una bomba de calor de agua a agua para agua caliente sanitaria (ACS) de con diferentes modos de trabajo. Sin embargo, se observa una degradación en el rendimiento global cuando se produce un fenómeno en el evaporador, llamado mala distribución. La mala distribución es la distribución no uniforme del caudal másico de refrigerante en un intercambiador de calor. Esto significa que diferentes zonas sobrecalentadas están presentes a lo largo del intercambiador de calor disminuyendo la transferencia de calor local que conduce a una degradación del COP. La temperatura no uniforme presente en la pared del evaporador debido a este efecto se puede registrar mediante una cámara termográfica.

Para comprender el problema mencionado, se realizó un análisis experimental de la distribución de refrigerante en un evaporador de placas en función de las condiciones de entrada (título de vapor) y salida (sobrecalentamiento) para diferentes diferencias de temperaturas en el fluido secundario. Para cada prueba, se toma una imagen termográfica de la superficie del intercambiador. A partir de los resultados obtenidos, se trata de caracterizar el fenómeno de la mala distribución y así ayudar en el diseño de este tipo de aplicaciones.

Palabras clave: bomba de calor, recuperación de energía, mala distribución de refrigerante, evaporador de placas soldadas, termografía infrarroja

RESUM

Els bescanviadors de calor de plaques soldades s'usen àmpliament en moltes aplicacions industrials a causa de la seua alta eficiència, compacitat i rendibilitat. Per a aplicacions de recuperació de calor en bombes de calor, per exemple, la diferència de temperatura en el fluid secundari pot ser superior als utilitzats en altres aplicacions (al voltant de 5 K). Amb la finalitat de trobar la millor estratègia per a extraure la màxima quantitat d'energia d'aigües residuals amb el millor rendiment global, el projecte europeu "Next Generation of Heat Pumps working with Natural fluids" (NXTHPG) centra tota la seua atenció a construir un prototip d'una bomba de calor d'aigua a aigua per a aigua calenta sanitària (ACS) d'amb diferents maneres de treball. No obstant això, s'observa una degradació en el rendiment global quan es produeix un fenomen en l'evaporador, anomenat mala distribució. La mala distribució és la distribució no uniforme del cabal màssic de refrigerant en un intercanviador de calor. Això significa que diferents zones sobrecalfades estan presents al llarg del intercanviador de calor disminuint la transferència de calor local que condueix a una degradació del COP. La temperatura no uniforme present en la paret de l'evaporador degut a aquest efecte es pot registrar mitjançant una càmera termogràfica.

Per a comprendre el problema esmentat, es va realitzar una anàlisi experimental de la distribució de refrigerant en evaporador de plaques en funció de les condicions d'entrada (títol de vapor) i eixida (sobrecalfament) per a diferents diferències de temperatura en el fluid secundari. Per a cada prova, es pren una imatge termogràfica de la superfície del intercanviador. A partir dels resultats obtinguts es tracta de caracteritzar el fenomen de la mala distribució i així ajudar en el disseny d'aquest tipus d'aplicacions.

Paraules clau: bomba de calor, mala distribución de refrigerant, evaporador de plaques soldades, termografía infraroig

ABSTRACT

Brazed plate heat exchangers are widely used in many industrial applications due to their high efficiency, compactness and profitability. For heat recovery applications in heat pumps, for example, the temperature difference in the secondary fluid may be greater than those used in other applications (about 5 K). In order to find the best strategy to extract the maximum amount of wastewater energy with the best overall performance, the European project "Next Generation of Heat Pumps working with Natural fluids" (NXTHPG) focuses all its attention on building a prototype of a water-to-water heat pump for domestic hot water (DHW) with different working modes. However, degradation in overall performance is observed when a phenomenon occurs in the evaporator, called maldistribution. Maldistribution is the non-uniform distribution of the mass flow of refrigerant in a heat exchanger. This means that different superheated areas are present along the heat exchanger decreasing the local heat transfer that leads to a degradation of the COP. The non-uniform temperature present on the evaporator wall due to this effect can be recorded by a themography camera.

To understand the problem mentioned, an experimental analysis of the distribution of refrigerant in a BPHE was performed based on the conditions of inlet (vapor title) and outlet (superheat) for different temperature glides in the secondary fluid. For each test, a thermographic picture of the surface of the exchanger is taken. Based on the results obtained, it is about characterizing the phenomenon of maldistribution and thus helping in the design of this type of applications.

Keywords: heat pump, DHW, refrigerant maldistribution, BPHE, infrared thermography, IR

TABLE OF CONTENT

TABLE OF FIGURES

TABLE OF TABLES

NOMENCLATURE

BPHE	Brazed plate heat exchanger	SC	Subcooling
COP	Coefficient of Performance	SH	Superheat
DHW	Domestic Hot Water	UPV	Polytechnic University of València
EU	European Union		
HX	Heat exchanger	T_{evap}	Evaporation temperature
ISE	Institut für Solare Energiesysteme	x	Vapor quality
MHX	Microchannel heat exchanger	DT/dT_w	Water temperature drop/ glide
MUTEDS	Master's Degree in Energy Technologies for Sustainable Development		
NXTHPG	Next Generation of Heat Pumps working with Natural fluids		
R290	Propane		

CHAPTER 1. INTRODUCTION

The present work belongs to a Master Thesis of the MASTER in Energy Technologies for Sustainable development (MUTEDS) from Polytechnic University of València (UPV), performed in the installation of the Institute for Energy Engineering (IIE) in collaboration with Fraunhofer-Institut für Solare Energiesysteme (ISE). This Master Thesis is framed within the EU project "Next Generation of Heat Pumps working with Natural fluids" (NXTHPG).

1.1 MOTIVATION

For centuries, our activities were provided by fossil fuels, but its negative environmental impacts are no longer acceptable. In order to stop (or diminish) Global Warming, CO_2 emissions need to be reduced to zero until the half of the 21th century. The need for a full decarbonisation of our activities on Earth, i.e. economical, residential and transport activities, is implied.

The energy usage in buildings are responsible for approximately 40% of energy consumption and 36% of CO2 emissions in the EU. Regarding the European Union (EU), the energy usage for heating in household represents a 65% while water heating represents a 14,5% [1,2]. Thus, buildings have a great contribution to Global Warming being its decarbonisation an important objective. While heating demands are expected to reduce within the next years by NZEB standards with better insulation and airtightness, domestic hot water (DHW) requirements will stay unmodified and must be produced in a more efficient and less pollutive way. Even energy can come from wastewater from own household. This idea is represented in the following Figure 1 and commented below.
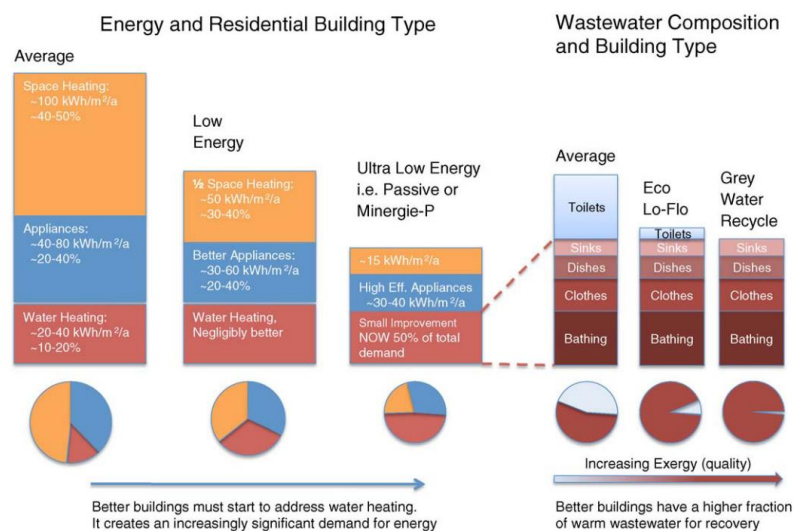
Figure 1. NZEB concept: the energy usage and wastewater recovery fractions [3]

Conventional heating system rely in fossil fuels either using a boiler or a solar thermal installation with a fossil fuel-based back-up. Electric boilers are low efficient and contributes to CO_2 emissions. The need for a highly efficient and low CO_2 emissive technology for hot water applications is mandatory if climate change plans like European 20/20/20 want to be accomplished.

Heat pumps (HP) are nowadays in a growing interest as an alternative to conventional heating systems. EHPA statistics state a progressive growing of this technology as shown in Figure 2, highlighting the increasing importance of two sectors: domestic hot water and exhaust air heat pumps in Figure 3. Domestic hot water heat pumps experimented an important growth in the EU over the past 7 years, reaching similar growth of Chinese market, while this segment is leading in Japan with ECO-CUTE since its introduction in the market in 2001 [4].
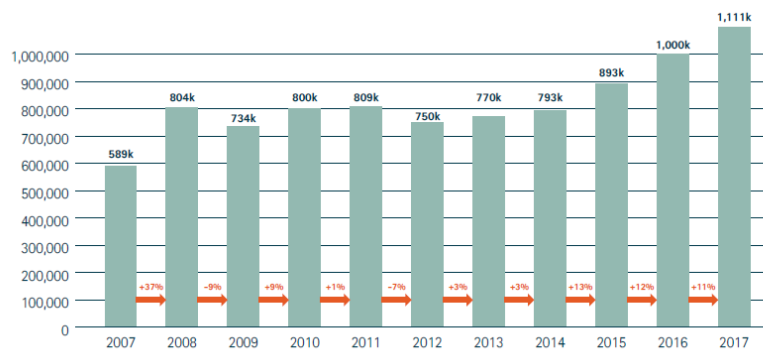
Figure 2. Heat Pump sales in the EU from 2007-2017 [5]
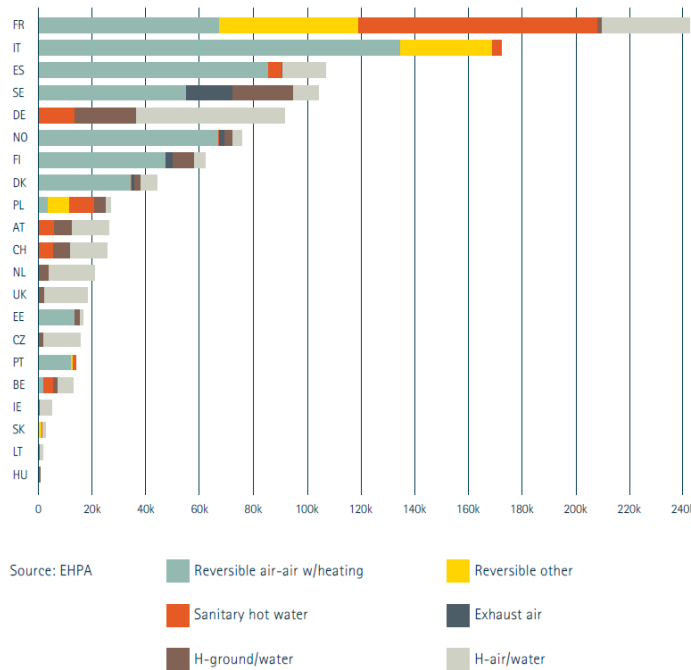
Figure 3. Heat Pump technology installations in EU [5]

Because of energy structures and environmental protection policies in westerns countries, wide researches in new heat recovery applications, such as heat recovery from the sewage water in residential sectors or condensing loops of commercial/industrial sector, are gaining importance within HP's. This source has usually higher temperature than ambient air, becoming an important and stable heat source for e.g. DHW and provide water to a tank for later user demand. Sewage water flow is function of the number of inhabitants and its habits. Hence, high or at least different temperature differences at the secondary fluid in the evaporator take place, as this source is not unlimited [6]. However, this issue needs further research and understanding [3][7][8].

In common heat pumps application, superheat is never recommended and only suggested for compressor reliability. However, in one hand, in heat recovery applications, extract the most energy as possible is worth doing and can be achieved by an optimum degree of superheat without decreasing the evaporation temperature. On the other hand, the phenomenon of maldistribution may appear and the application of superheat do not lead to an improvement and performance of heat pumps decreases. This is being explained in chapter 3 with more detail.

As mentioned, water heating in households represents a big share and is provided to many uses: shower, dishwashers, clothes washers, etc. Wastewater (sewage) retains an important amount of its initial energy and could be recovered. From Swiss studies [9] the 15% of the energy supplied to a building is lost via sewage water. Therefore, in the 1990's, Switzerland observed the high potential of this available source and started a program to improve and take profit of wastewater. While this source is being used for heating and cooling for many years by Scandinavians in Europe, Europe is improving in technologies and strategies for heat recovery from wastewater due to the related problems concerning the whole world.

Wastewater has the following aspects that makes this source profitable:

- Wastewater temperature is almost constant all over the year and higher than ambient air temperature [6], justifying thus, better performance of water source heat pumps than air source heat pumps.
- The main disadvantage is that sewage is a finite source of energy and not everywhere available, but the water amount is high enough in industry, hospitals and buildings states. However, water quantities and availability must be carefully analysed [10].
- Flow rate is stable and almost constant but is depended of consumer habits: water flow at nights is lower than within the day [6].

In order to fulfil Montreal, Kyoto and F-Gas protocols, natural refrigerant, such as CO_2 and hydrocarbons, are best candidates for heat pumps in DHW applications. After the 1930s, CO_2 has been substituted by synthetic refrigerants. For the revival of CO_2 in refrigeration systems, the remarkable works of Lorentzen et. al [11,12] and Nekså et al. [13,14] played an important role. These studies proved that the use of this refrigerant can meet the needs of water heating operating at transcritical region and is a good replace for conventional refrigerants. Further studies care about the optimization in CO_2 HP for domestic hot water (DHW) production by controlling the gas cooler pressure by means of water inlet temperature and have shown high efficiency [15,14]. Nevertheless, in DHW applications where temperature lifts in the secondary fluid at the condenser may be above 50 K, it is not possible to set the optimum rejection pressure due to an internal pinch point i.e the water temperature along

the gas cooler limits the refrigerant temperature profile. Therefore, a numerical approach calculates the optimal pressure depending on the inlet and outlet temperatures of the secondary fluid thus, the maximum performance can be adjusted at any external condition [16].

Whereas CO_2 has been proved in the last decades to be suitable for DHW applications, hydrocarbons are available too. Commercial heat pumps like Quantum [17] uses propane (R290) as refrigerant. Quantum heat pump model heats up water in sequences of temperature lifts of 5 K. The main disadvantage is that the heat pump is not able to supply the demanded water temperature (60ºC) directly as CO_2 heat pumps and benefits of subcooling are not employed [18]. Researchers observed improvement with a certain degree of subcooling in subcritical cycles although the value of subcooling is not indicated [10,14]. More directly, many studies focus on finding an optimum subcooling [15,16]. Nevertheless, these works focus on low temperature lifts where the optimum subcooling is between 5 and 10 K. European Project Next Generation of Heat Pumps working with Natural fluids (NxtHPG) [22] is aware of the importance of using natural refrigerants and centred attention in propane. Within this project framework, the optimization of subcritical cycles using propane were published [18,19] in which they analyze the effect of subcooling over the HP performance. Further NxtHPG studies in subcooling [25] showed that there is an optimum value and it mainly depends on the temperature difference between the inlet and the outlet of the secondary fluid in the condenser. A temperature lift of 50 K (from 10ºC to 60ºC), such as in SHW applications, the optimum subcooling is 46 K while for a 10 K temperature lift (from 50ºC to 60ºC) it is 8,8 K. The degree of improvement regarding the cycle without subcooling is 35% and 8,5% respectively. The optimization of the degree of subcooling can lead to better COP than CO_2 cycles is concluded. Further studies comparing both refrigerants, showed for low water temperature inlet, better COP for CO_2 cycle whereas after a certain value of the water inlet temperature, the R290 subcritical cycle (without subcooling) showed better results [26].

HP's with natural refrigerant CO_2 is leading the increasing market of HP for DHW applications and is substituting conventional refrigerants. However, as there exists an optimum value of subcooling for R290 HP for different temperature lifts in the secondary fluid and presents better COP when water inlet temperature is high, this kind of HP could be more competitive if the heat pump works heating up water sequentially and with an adequate value of subcooling.

In common heat pumps application, superheat is never recommended and only suggested for compressor reliability. However, in heat recovery applications, extract the most energy as possible is worth doing and can be achieved by an optimum degree of superheat without decreasing the evaporation temperature. This is being explained in chapter 3 with more detail.

1.2 OBJECTIVES

Heat pumps (HP) are nowadays in a growing interest as an alternative to conventional heating systems (e.g. boilers or solar thermal installations) as the EUROPEAN DIRECTIVE 2009/28/CE states important SEASONAL PERFORMANCE FACTORS (SPF) for Domestic Hot Water (DHW) applications. The best performance of heat pumps under variable and/or extreme conditions must be considered, e.g. when heat sources are not continuous or limited. The main aim of this work is to improve the working performance of heat pumps for heat recovery solutions and study issues or problems that appear while its operation.

To fulfil the objective the following activities have been performed within this thesis:

- Undertake an open literature review analysis and contrast obtained results.
- Understand and be able to manipulate a water-to-water heat pump (WWHP) developed in the EU Project NxtHPG for DHW applications changing superheat (SH) and subcooling (SC) with PID control.
- Investigate the possible issues that decreases the performance of the WWHP under different inlet and outlet conditions during the working of the heat pump.
- Compare experimental results with *IMST-ART software,* a simulation tool to assist the selection, design and optimization of refrigeration equipment and components.
- Observe the maldistribution phenomenon with infrared thermography (IR).
- Propose innovative model and explanation for maldistribution from the observations made.
- Contribute to the research field with a new contribution.
- Apply the knowledge and formation gathered during my bachelor and master's degree.

1.3 LIMITATIONS

The WWHP uses propane (R290) as refrigerant. The observations made can only be stated for the mentioned HP and cannot be generalized for other refrigerants. Thermodynamic properties are specific for each refrigerant and maldistribution could be observed or not for other refrigerants. However, deeper study in this topic should be progressed.

1.4 ORGANIZATION OF THE THESIS

This section is a guide for the reader to examine this document carefully by outlining the chapters and points discussed. The work is split in five chapters: Introduction, Literature Review, Justification, Methodology and Obtained results and analysis and Conclusions. For further information or detail, please refer to the bibliography when mentioned.

The first chapter provides a general description of how heat pumps are being introduced in the market and for what are they starting to be demanded. Its importance for wastewater is stated. The performance in this technology done within the last years claim heat pumps to be important in the next years and description of observations made and lead to this thesis. Objectives and limitations are stated.

Chapter 2 provides a background review of useful literature important for the study were also examined: concept of maldistribution, its disadvantages and how it can be avoided. Manufactures are continuously struggling with improving maldistribution while researchers are trying to define it with mathematical or analytical models. However, trying to study maldistribution within different working conditions are not explicitly addressed.

Chapter 3 gives a brief description of observations made and lead to this thesis: a general performance drop when superheat was applied. This disagrees with the expected theory and simulation studies. A pinch point analysis states the reasons why superheat should be applied.

Chapter 4 presents the test rig, its components, instrumentation, test matrix and how the experimental campaign was carried out. The commercial software used is presented with examples and how data was introduced.

Chapter 5 presents the obtained results of the experiments and its representative thermography. A comparison between simulation tool and experimental results. Evaporation temperature is the parameter that is analysed. An innovative model of an evaporator by separating it into two smaller subexchanger is presented and with an analysis of the size of the evaporator used in the application, maldistribution can be explained.

Chapter 5 gives the conclusion of the study and provides an insight into possible further studies.

CHAPTER 2. LITERATURE REVIEW

The aim of this chapter is to introduce the reader into the aspects related to the performed work. A brief state of art of these different subsections can be found:

- Significance of maldistribution problems
- Maldistribution quantification and observation
- Numerical and simulations studies
- Avoid maldistribution by improvement strategies

Firstly, studies that have studied the importance of two-phase flow maldistribution in evaporators is outlined. The reader should understand that maldistribution is mainly a problem related with evaporators as two-phase flow is entering and difficult to handle.

The next part focuses on how authors tried to understand and quantified refrigerant maldistribution. The best way and therefore non-intrusive and non-destructive, maldistribution can be observed as non-uniform surface temperature in evaporators by IR thermography. Other authors observed two-phase flow pattern at the entry has been observed and stated a direct influence in maldistribution.

Numerical or analytical studies are performed and discussed in the following part. Condenser related studies were found but will not be discussed in this thesis.

Finally, new approaches suggested in open literature and manufactures to avoid maldistribution is presented. Different strategies and the resulting system performance are discussed.

2.1 SIGNIFICANCE OF MALDISTRIBUTION PROBLEMS

As before mentioned, heat pump can be advantageous compared with other conventional technologies. However, performance degradation could occur due to the occurrence of refrigerant maldistribution. Maldistribution was quickly observed as higher demands and bigger heat exchangers (HX) were needed. Simulation tools assume uniform refrigerant flow through channels or tubes but in real systems, maldistribution is always present in some amounts. Evaporators are sensitive to uneven distribution of liquid and vapor. Heat transfer is highly degraded in liquid-lacking channels: heat transfer coefficient is lower for single-phase vapor flow regarding two-phase flow and as the refrigerant superheats, the temperature difference between refrigerant and the secondary fluid (e.g. water) reduces. Figure 4 shows the issue that this document is trying to understand for a brazed plate heat exchanger (BPHE). Maldistribution for other kind of HX is different as air-side maldistribution can occur. Furthermore, surface temperature is not distributed uniformly and can be observed by infrared thermography. Due to maldistribution, liquid or droplets can quite the evaporator and have an influence in the thermal expansion valve control. All these problems lead to a degradation in the

performance of the system i.e. significant reductions in cooling capacity and COP. Thus, this is an important area of study and worth focusing into when seeking for improvement of heat exchangers.
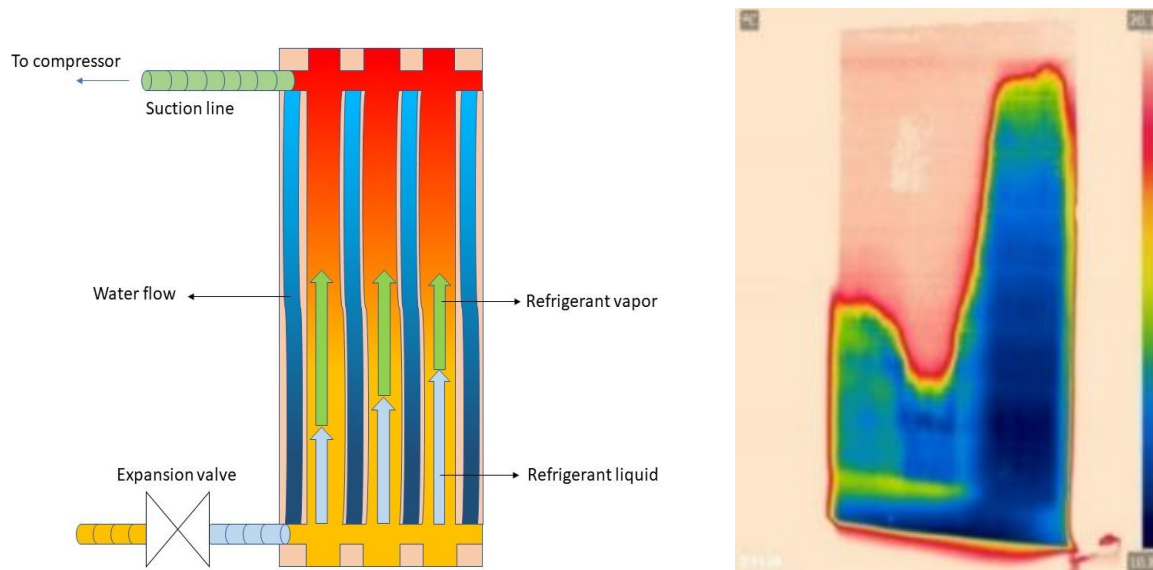
Figure 4. Uneven distribution of refrigerant in heat exchangers is observed with thermography as unequal distribution of wall temperature

2.2 MALDISTRIBUTION QUANTIFICATION AND OBSERVATION

Visualization of the phenomenon is being explored by many authors. Sometimes the phenomenon can be observed by the naked eye as in Figure 5. Otherwise, there are mainly two approaches. The first one, follows the idea of the ice deposit and temperature observation of the surface, is non-intrusive and has no effect on the experiment set-up and the refrigerant: infrared thermography. The second is using both transparent tube and/or HX header and observe the directly the mass flow and its flow pattern. The second approach is likely to have influence in the experiment as the transparent material has different roughness compared to tube material.

Figure 5. Ice deposit on outside of the BPHE

While [27, 28] used infrared thermography technology to observe and measure wall temperature to estimate heat transfer coefficients, maldistribution is noticed in its pictures. [29] took profit of IR to picture the distribution of refrigerant in a microchannel HX. Tube wall temperature can be related with mass flow through each tube. The approach was validated against experimental method and showed high accuracy. Following the same approach, [30] developed a statistical method to quantify both refrigerant maldistribution and the correct used evaporator area for evaporation.

Flow visualization through a transparent tube, header or manifold offer a better insight in mass flow maldistribution. [31] studying the effect of the evaporator orientation and its consequences in mass flow distribution for microchannel HX, a transparent inlet header was installed. For the orientation with vertical upward flow, a stratified flow pattern was observed, and liquid lacking channels were observed in the first channels. Neither mass flux nor inlet quality were stated.

Two phase flow distribution were observed with twelve different manifolds varying inner diameter and number of vertical tubes by [32]. Mass flux and inlet quality are variables changed during the tests. Gas feeding of the first tubes were observed by the most part of the experiments.

Maldistribution is related with flow patterns and pointed out by many authors [33, 34]. Exhaustive work made suggest maldistribution is caused by the flow pattern. The tube after the expansion valve and the inlet header is observed with transparent PVC. Depending on mass flux and inlet quality as seen in Figure 6, the observed flow pattern is indicative of the refrigerant distribution. Low velocities and low vapor phase quantity imply a liquid jet that fills the first channels; medium inlet quality, a stronger jet reaches the end of the manifold and creating a pooling, filling with higher quantity the last channels or with high velocities, phase separation occurs in the jet and a front pooling occurs. Homogenous mist flow is rarely observed with high inlet quality and high velocity. The hole space is homogenously filled, and best distribution of refrigerant is observed. The following flow pattern and flow distribution is shown below.
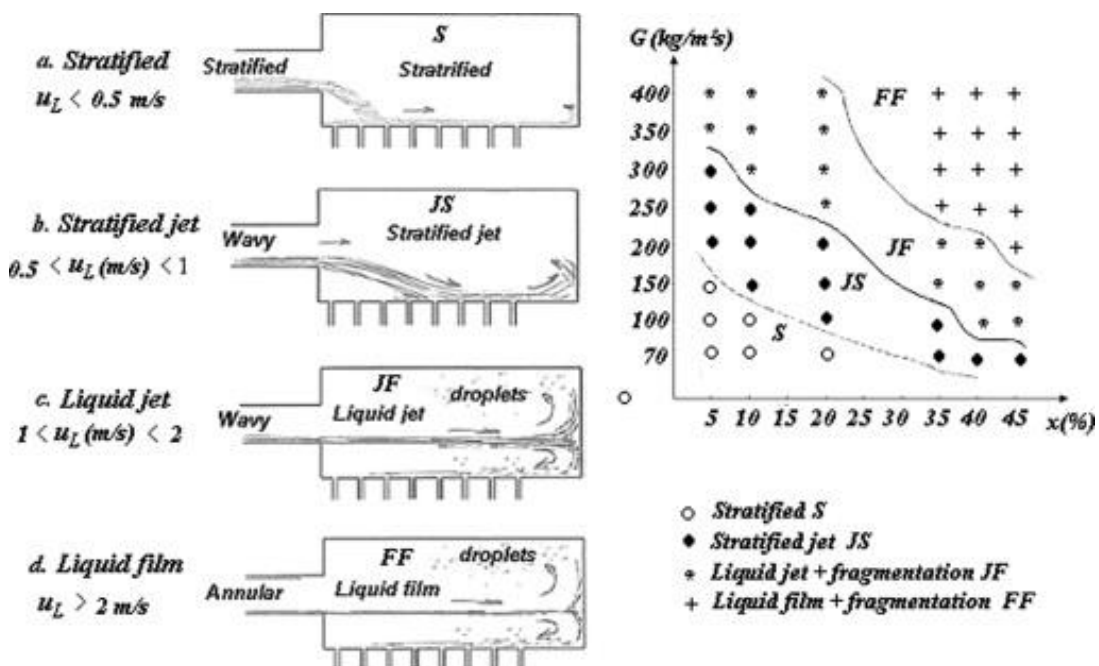

Figure 6. Flow structure in HX headers [35]

Mist flow is suggested by SWEP, BPHE manufacturer, as the best flow pattern but is rarely achieved as high quality and velocities are related [36].

2.3 NUMERICAL OR ANALITICAL STUDIES

From the early literature on the plates arrangements on flow distribution is presented [38,39] where results from an mathematical model study indicate that manifold diameter and number of channels have great influence in single-phase flow maldistribution. Thermal performance degradation depending on if it is a U-type or Z-type heat exchanger has been evaluated. Z-type plate arrangement have more tendency to suffer maldistribution [39]. U-type and Z-type arrangement is presented in Figure 7.
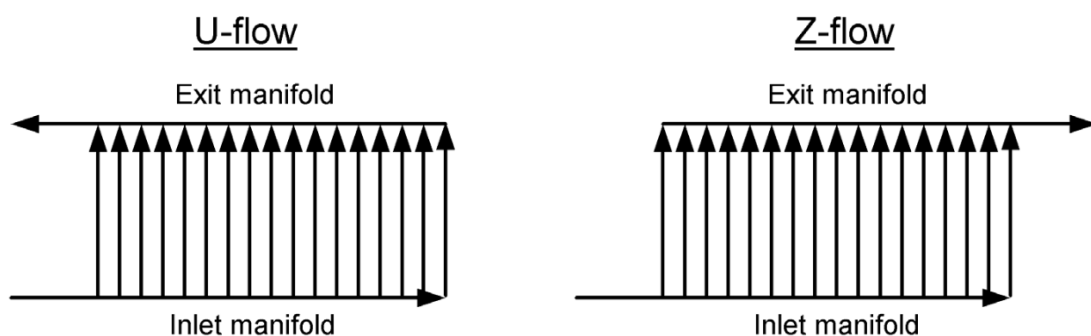
Figure 7. Channel flow distribution for U-type and Z-type heat exchangers [40]**.**

As before mentioned, IR pictures and flow visualization are manners of quantification but cannot give information about capacity loss and COP degradation. Authors tried to simulated systems numerically and analytically, representing maldistribution mathematically and translate maldistribution into performance degradation. Comparison of capacity and COP degradation depends on the severity of the initially chosen maldistribution by the authors.

A plate HX is simulated numerically by [41]. Quality distribution profile was supposed decreasing linearly from the entrance to the last channel. A 25% reduction of the U-Value can be expected by vapor quality maldistribution.

A mathematical model of a Microchannel HX (MHX) mas made by [42]. Quality distribution profile was supposed decreasing linearly from the entrance to the last channel, likewise [41]. The used refrigerants were CO_2 and R134a and explored the effects of air-maldistribution and uneven inlet quality on performance of the system. Air side maldistribution showed greater impact on performance. The maldistribution of CO_2 appeared less critical than R134a nonuniformity since there is less of a density difference between phases.

As for the difficulty of defining quality maldistribution, a more recent developed mathematical model evaluates the single-phase flow distribution in a brazed plate heat exchanger [43]. The model follows the principle of equal pressure drop for each flow path and has been validated with experimental results. Single-phase flow maldistribution is highly related with the pressure drop along the header

and the channels. Uneven distribution of flow is more severe as the number of plates increases and for the length of the plates decreases.

2.4 AVOID MALDISTRIBUTION BY IMPROVEMENT STRATEGIES

Maldistribution issues were solved by smart refrigerant distributors or HX redesigns of headers and tubes. These solutions are cost prohibitive and are not necessarily optimal under all working conditions. The simplest approach to decrease maldistribution influence is increasing the evaporator size in a finned and tube HX [44].

Maldistribution between the parallel channels of a heat exchanger can have impact in the overall performance. The refrigerant when leaving the expansion valve and entering the evaporator, the refrigerant is a mixture of liquid and vapor. Depending on the flow pattern, the two phases may divide differently. A distributor is installed at the inlet of each channel of evaporators, to avoid maldistribution. Commercially available evaporators have installed a distributor. There are distribution devices e.g. SWEP developed a reliable system that feeds homogenously with refrigerant all channels ensuring highly efficient heat transfer [45]. Other system devices that ensures refrigerant distribution in microchannel heat exchanger is presented by Danfoss and justified with thermography pictures as in Figure 8 and compared with a TXV control that is more usual in Figure 9. Refrigerant levels are high in all circuits with the proposed improvement by Danfoss and a clear maldistribution is observed with the TXV control [46].
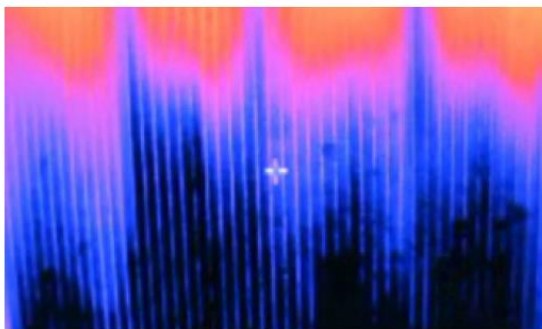
EcoFlow control

Figure 8. Thermography picture of a microchannel heat exchanger with refrigerant distribution control system [46]**.**
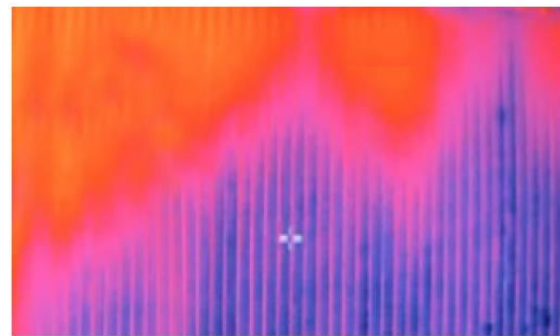
TXV control

Figure 9. Thermography pictures of a microchannel heat exchanger without distribution control [46]**.**

The importance of distributors has been observed by [40]. Five different evaporators have been tested under same boundary conditions i.e. superheat, vapor quality and saturation pressure, although it is not mentioned which were the values of these parameters. All evaporators count with the same heat transfer area and number of channels. The resulting heat transfer coefficients are rather different. Author suggests the importance of selecting the correct size and type of the distributor for the application.

Expansion orifices or splashing grids were tested by [35]. Expansion orifices produces a liquid jet that renders in a more homogeneous distribution. A splashing grid produces droplets in many directions improving the two-phase distribution. In Figure 10 the mentioned effects are exposed.
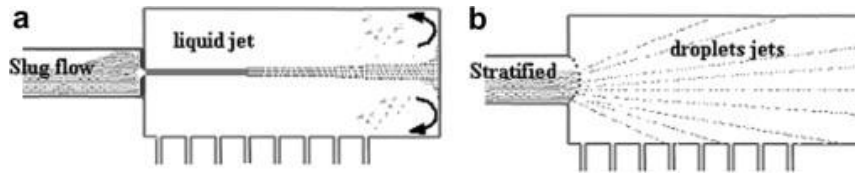

Figure 10. Flow patterns after the two expansion devices. (a) Expansion orifice and (b) splashing grid [35]

For microchannel heat exchangers, [29] proposed an improvement for achieving better refrigerant distribution. The solution consisted in remove flash gas; vapor phase is separated from liquid phase after the expansion valve. In this way, only liquid is flowing within the microchannel heat exchanger while the vapor phase is being bypassed. This is called flooded evaporator. Thermography pictures showed clear more uniformly distributed superheat with this flash gas removal system. Although the heat transfer increases in this way, the pressure drop on the refrigerant side was the dominant improvement, so better system performance was observed when using the separation device. However, 0K superheat test was not performed. SWEP agrees in using flooded evaporators as distribution improves as liquid is flowing at the entry [36].

2.5 CONCLUSIONS

From this literature review the following conclusions can be outlined:

- Maldistribution causes performance degradation in terms of U-value or COP.
- Different approaches are used to visualise maldistribution and have different influence in the experimental set-up. When using thermography there is no impact but other visualization strategies are intrusive.
- The influence of different process conditions like superheat or the temperatures difference at the secondary fluid for the two-phase flow evaporation are rarely or not addressed in literature.
- The most part of the literature focus on understanding the causes and effects of maldistribution and few of them try to control it.
- Manufactures are aware of this issue and try to develop systems that can control or decrease the effects of maldistribution.
- Literature deal with MHX being these evaporators widely used in both automotive and aeronautic sectors and PHE or BPHE are rare. However, this seems to be reflective of industry trends.
- Vapor phase is more likely to enter the first channels from performed experiments.
- Maldistribution is highly related with the flow pattern developed after the expansion valve and at the manifold. Velocity and inlet quality are parameters to take into account and have great effect on this phenomenon.

- Distributors and smart designs are not necessarily optimal under all working conditions.
- Mathematical models suppose the quality maldistribution linearly and are not realistic but can be useful for understanding the problem and its consequences.
- Only liquid entering is a general solution to avoid maldistribution as seen in flooded evaporators.

From these conclusions, in order to fully understand the reasons of the appearance of maldistribution under different working conditions more deeply, a measurement campaign by changing inlet and outlet conditions, thus inlet quality and superheat for a given secondary temperature difference. Uneven temperature distribution in the surface is a result of non-uniform refrigerant distribution within the channels and can be registered with a thermography camera.

CHAPTER 3. JUSTIFICATION

3.1 SUPERHEAT AND SUBCOOLING IMPROVEMENT STRATEGIES

Researchers are in continuous struggle improving heat pumps performance. In previous works performed by IIE the water-to-water heat pump that is under study in this thesis has been designed with different working modes and trying to achieve maximum COP by the improvement of subcooling.

It was justified from a pinch point analysis, an optimal subcooling performed in the condenser can be beneficial and lead a general performance that is competitive with the achieved by CO_2 transcritical heat pumps [25]. When the refrigerant is capable to reach as close as possible the secondary fluid temperature at any point of the heat exchanger, the maximum heat is being transferred. In the mentioned heat pump of the European project: "Next Generation of Heat Pumps working with Natural fluids" (NxtHPG), the working performance increased significantly, and the expected results were obtained. However, for the case of the optimum degree of superheat applied in the evaporator to achieve higher COP, as stated by an exergetic analysis, was never acquired. However, the analysis showed that setting a superheat below the optimum, had not significant effect on the performance of the components.

The main objective was to analyse the effect of superheat on the performance for heat recovery applications. From the exergetic analysis, an optimal superheat was found based on the temperature of the secondary fluid. Although the optimal superheat does not lead to a higher overall performance but a control similar to the implemented with subcooling could be worthy in application were secondary fluid temperature glides are high.

There existed a disagreement between theoretical expectations and experimental tests. From theory, using IMST-ART software, simulation tool for the analysis for heat pumps, the existence of an optimum degree of superheat for different secondary temperature difference was expected. From the test results, higher performances are always obtained with low or zero superheat. Figure 11 shows experimental results and theoretical performance variation with secondary temperature difference for 0 K and 10 K superheat. Water inlet temperatures at the evaporator were changed and made for 35ºC, 20ºC and 15ºC for constant conditions at the secondary fluid lift at the condenser, from 20ºC to 60ºC. Blue and dashed green lines belong to 10 K and 0 K superheat theoretical performance respectively while blue triangles and orange points belong to 10 K and 0 K superheat experimental results respectively.
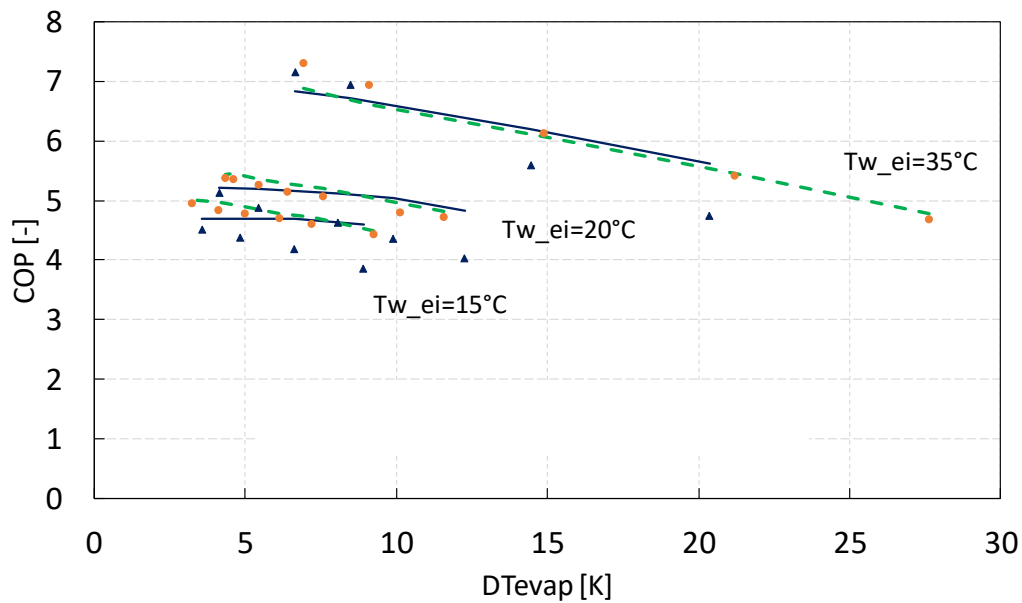
Figure 11. Experimental results and theoretical performance with the secondary temperature difference at the evaporator for zero superheat (0K1V) and 10 K (10K2V).

As an example, the COP reduction for water inlet temperatures at 20ºC between zero superheat and 10 K superheat are presented in the next Table 1.

Table 1. Performance comparison for zero and 10K superheat

dT [K]	COP (SH=0)	COP (SH=10)	COP Reduction %
4.08	5.21	5.13	1.50
5.30	5.18	4.84	6.56
7.61	4.99	4.56	8.65
11.57	4.73	3.99	15.66

Far from the expectations from theory, working with a degree of SH is reducing the general performance of the heat pump. For low water temperature glides, the reduction is negligible but becomes more noticeable as the water temperature glide increases. Any possible benefit that was expected to obtain with using SH must be avoided.

Similar discrepancies were obtained for evaporating temperatures and the main refrigerant cycle characteristics in the evaporator. An unexpected evaporation temperature drop happened. For several experimental results with different degree of superheat is presented in Figure 12. Evaporating pressure and temperature variation with the water temperature glide at the evaporator for different

superheats. Therefore, the looking for an explanation, the observation of the refrigerant distribution in the evaporator was performed.
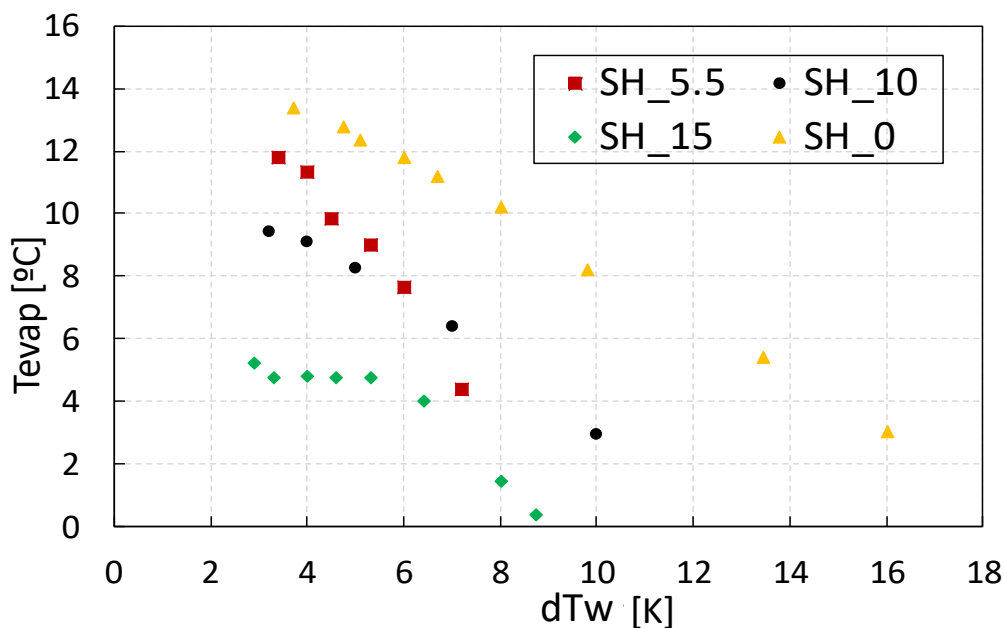

Figure 12. Evaporating pressure and temperature variation with the water temperature glide at the evaporator for different superheats

Regarding the work performed in this master thesis, it emerges from the observations made by IIE and a detailed study is needed to find an explanation and condensed in this work. This research line follows operating the same WWHP and is being performed in collaboration with the Fraunhofer-Institut für Solare Energiesysteme ISE.

3.2 PINCH POINT ANALYSIS

In order to explain from a thermodynamically point of view the importance of doing superheat is explained with the Pinch Point analysis.

A heat exchanger is used to transfer heat from a fluid to another. The maximum heat transfer is achieved when the used heat exchanger has an infinite conductance (UA or NTU $\rightarrow \infty$). The temperature difference between both fluids will approach zero somewhere within the heat transfer process. The location where the temperature is smallest is referred as Pinch Point.

As explained in [25], when double pinch point is achieved, the better performance of the condenser, existing three phases throughout the condenser. For the case of an evaporator, considering two-phase flow at the entrance, best performance requires two pinch points too, one at the entry and the other at the outlet as seen in Figure 13. Desirable temperature distribution of water and refrigerant at the evaporator.
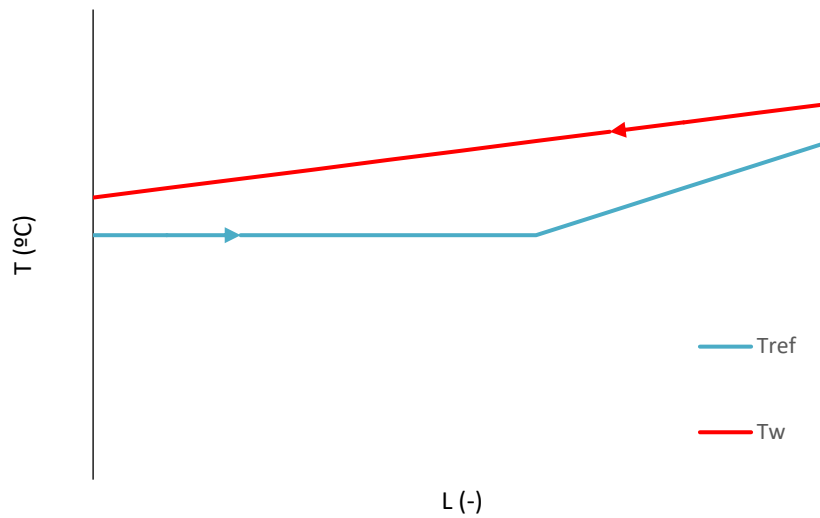
Figure 13. Desirable temperature distribution of water and refrigerant at the evaporator

Considering best performance of an evaporator when double pinch point is achieved, the existence of an optimum SH is considered. To proof the existence of an optimum SH, the assumption of an infinite heat transfer area is considered. Performing a parametric study with IMST-ART simulation tool, changing water temperature drop and degree of superheat. Inlet quality has been set fixed. The evaporator area is oversized and will work with infinite conductance.

In the next Figure 14. ΔT_1 and ΔT_2 for different dTw and SH the pinch point at the entry (ΔT_1) and at the outlet (ΔT_2) are plotted with water temperature drop and superheat in the axes.

Figure 14. ΔT_1 and ΔT_2 for different dTw and SH
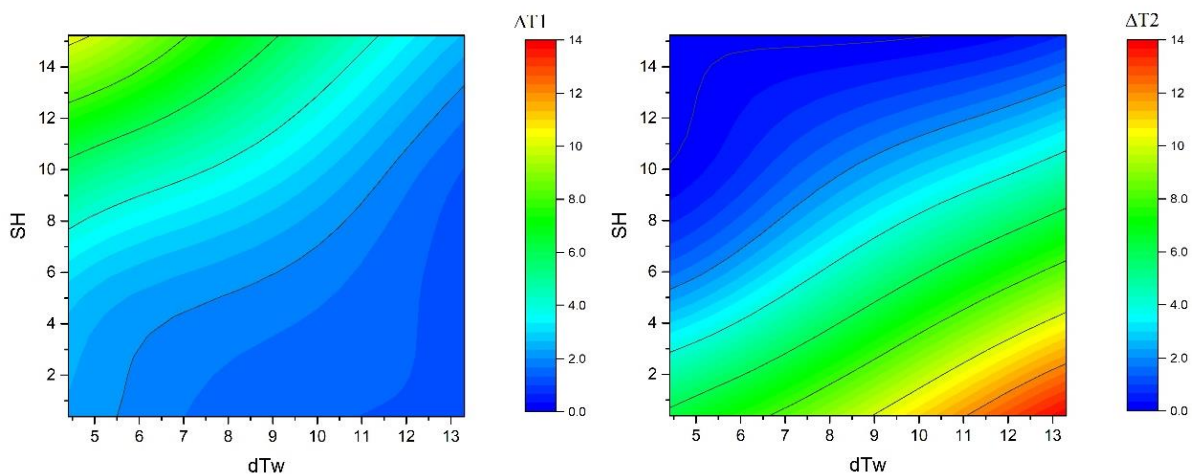
As stated and can be observed, Figure $_{14.}$ $\Delta T1$ $_{and}$ $\Delta T2$ for different dTw and SH, when no superheat is applied, ΔT_1 will be almost zero being almost the same evaporation temperature and outlet

temperature of the secundary fluid whereas for superheat applications, the evaporation temperature will be below outlet water temperature increasing so the ΔT_1. The opposite occurs for ΔT_2 being this difference the smallest for applied superheat and the highest when zero superheat is used. When the dTw increases, to achieve a smaller ΔT_2 a higher SH must be applied.Figure 15 and Figure 16 shows the explanation.
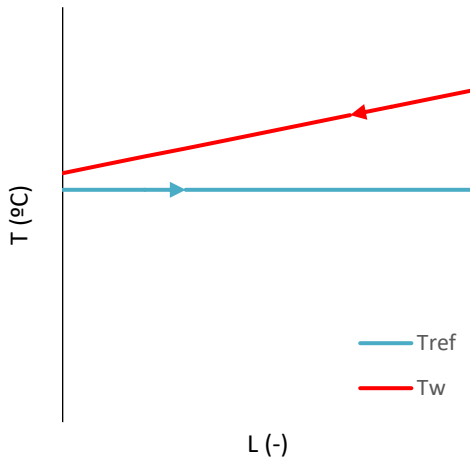
Figure 15. Refrigerant temperature matches water outlet temperature for zero SH
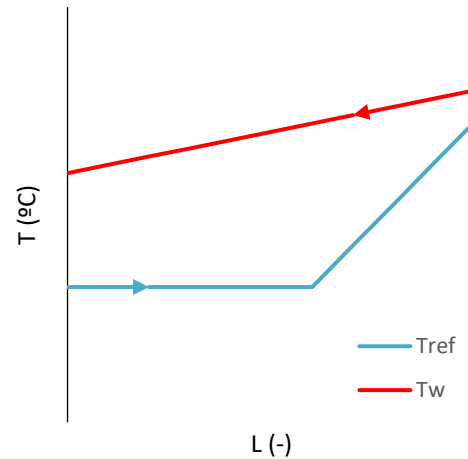
Figure 16. Refrigerant temperature matches water inlet temperature for a certain SH

In the following Figure 17. The sum of ΔT_1 and ΔT_2 for different dTw and SH ΔT is the sum of ΔT_1 and ΔT_2. The smaller values for ΔT the better performance of the evaporator. There is a zone in blue that corresponds with the best performance of the heat exchanger and placed in SH applications. SH is normally applied for system reliability in order to not degrade the compressor but is never justified as an increase of the maximum heat exchange rate.
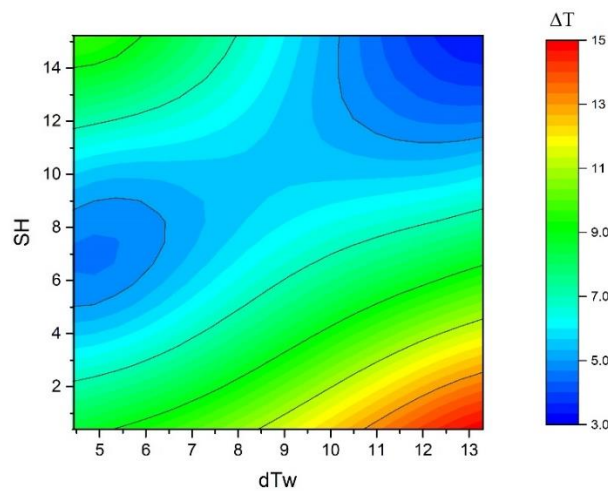
Figure 17. The sum of ΔT_1 and ΔT_2 for different dTw and SH

In an evaporator used in heat pumps, the cold fluid is the refrigerant whereas the hot fluid is air or water. Refrigerant enters the evaporator in two-phase flow, being the optimum evaporation temperature the outlet temperature of the hot fluid. However, when superheat is applied the evaporation temperature is restricted to the difference between inlet secondary fluid temperature and mentioned superheat, only when it is higher than secondary fluid temperature drop. From the before explained Pinch Point concept, the smallest temperature difference between the secondary fluid is achieved at the entrance when SH is zero while for SH conditions (where $dT_w < SH$), this small difference is achieved at the outlet. The maximum evaporation temperature considered follows the expression as in (1):

$$T_{evap} = T_{w_{in}} - \max{(dTw, SH)} \tag{1}$$

Therefore, when SH equals dTw, the pinch point is achieved at both entry and outlet. From this analysis we can state as a rule of thumb the best performance of the evaporator is obtained by the optimum SH and is equal to the secondary fluid temperature glide as stated in (2):

$$SH_{opt} = dT_w \tag{2}$$

CHAPTER 4. METHODOLOGY

This chapter introduces the WWHP system. The WWHP prototype allows working in two modes: one with a zero SH control and a variable SC and other with both variable SH and SC. A variable SC control allows a different inlet quality at the evaporator. Therefore, SH and inlet quality can be evaluated as affecting parameters in maldistribution.

As mentioned in the introduction chapter, a better performance with SH is expected. This is being discussed in this chapter and justified with a Pinch Point analysis. The concept of an infinite area HX is applied.

Disagreement with simulation software and experimental results are expected to happen due to refrigerant maldistribution. As introduced in the literature review, maldistribution can be observed with IR. When refrigerant flows unevenly through the HX, temperature distribution of the surface reflects the refrigerant distribution. Description of the test campaign is given.

4.1 TEST RIG DESCRIPTION
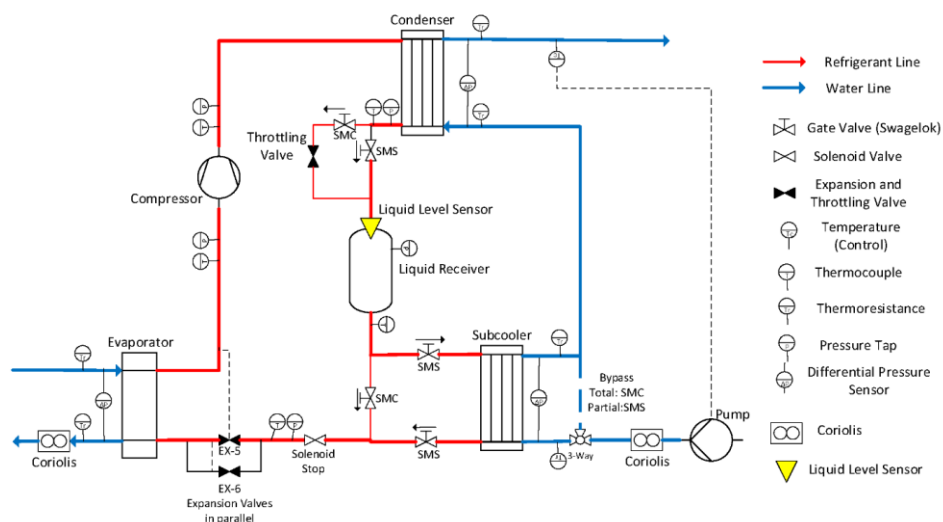
Figure 18. Propane Water-to-water heat pump booster

The study is performed in a WWHP with R290 as refrigerant. The developed heat pump (Figure 18), the prototype of the European project 'Next Generation of Heat Pumps working with Natural fluids' (NXTHPG), although working with the same components as a common heat pump, is able to work with three different configurations: **MODE A, MODE B** and **MODE C**. **MODE A** configuration is not being

utilised in this study. Further information about the heat pump and its configurations can be found [47].

Table 2 shows the main components of the prototype:

Table 2. Characteristic of the components of the HP system

Component	Type	Size
Compressor	Scroll (2900rpm)	$29.6m^3h^{-1}$
Condenser	BPHE Counter-flow	3.5m2
Evaporator	BPHE Counter-flow	6m2
Liquid receiver	-	8 l
Expansion valve	Electronic EX-6	93 kW
Throttling valve	Electronic EX-5	39 kW

Figure 19 shows the lay-out and the refrigerant cycle of MODE C configuration. As it can be seen in the diagram, the liquid receiver is placed at the outlet of the evaporator fixing the superheat at 0 K during the performance of the heat pump. The expansion valve controls subcooling instead of superheat. This configuration permits to adapt the subcooling to the external condenser conditions resulting in an improvement of COP [25].
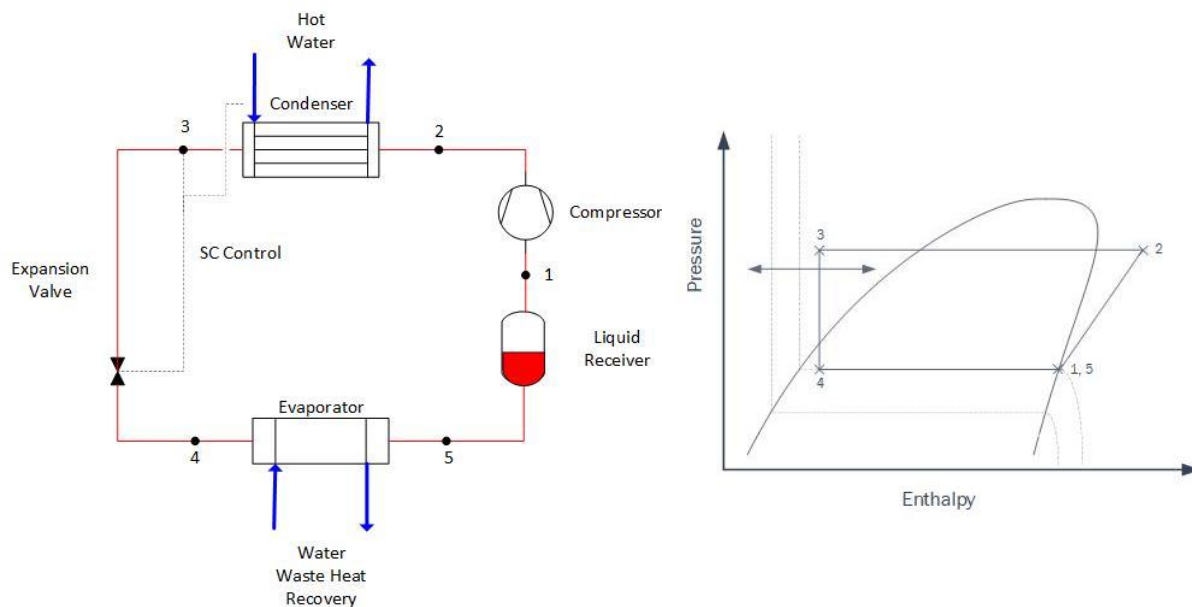

Figure 19. MODE C configuration: system lay-out and thermodynamic p-h diagram

Figure 20 shows the MODE B configuration, in which the heat pump can control subcooling in the condenser and superheat in the evaporator independently with two electronic valves. A throttling valve, located between the condenser and the liquid receiver and an expansion valve, places between the liquid receiver and the evaporator. Subcooling setting at the condenser is controlled by the throttling valve and superheat setting is controlled by the expansion valve. The liquid receiver is in charge of accommodate changes in the active charge in the system due to variations in superheat and subcooling.
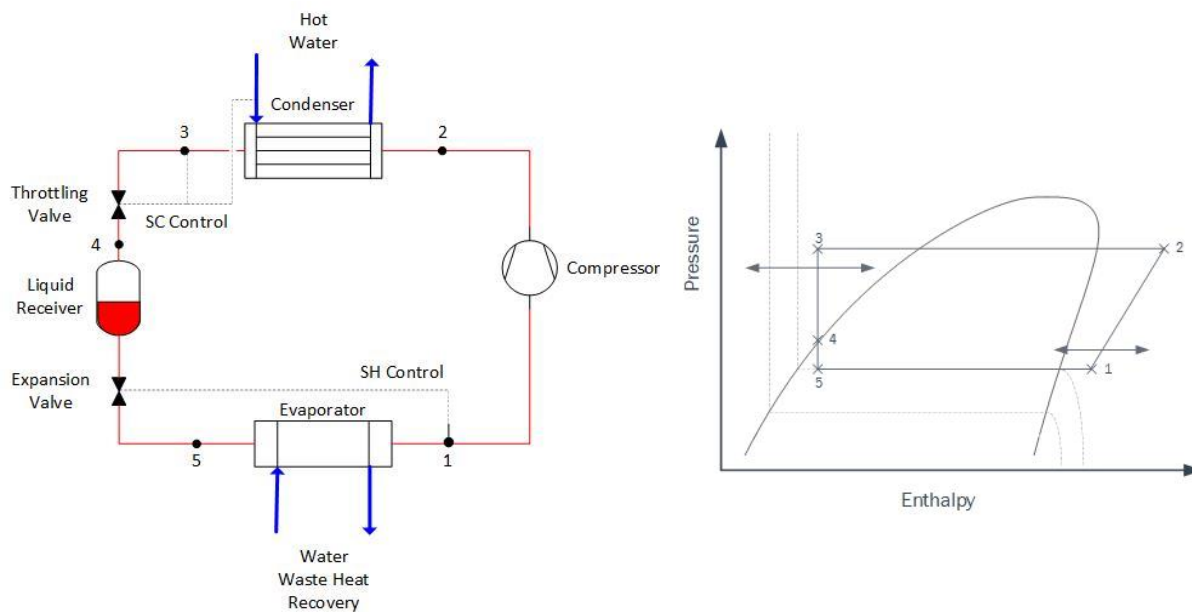

Figure 20. MODE B configuration: system lay-out and thermodynamic p-h diagram

The aspect of no-superheat control is being evaluated. In common heat pump applications, such as domestic hot water (DHW) supply, superheat has inherited a negative effect on the performance and just small degrees of superheat is used to ensure compressor reliability. However, for heat recovery applications, large secondary temperature difference at the evaporator could be profitable, so a certain degree of superheat can be beneficial. Therefore, working in MODE C without superheat could contribute as a penalty to the efficiency of the system.

As before mentioned in Chapter 2, the performance is always greater when MODE C configuration is applied although the water temperature glide at the evaporator increases and better performance for MODE B was expected.

4.2 EXPERIMENTAL PROCEDURE

Based on the pre-evaluation and literature research on the relevant aspects a field of operation points was defined and characterized experimentally. The measuring points are plotted in figure 21 for a better understanding.
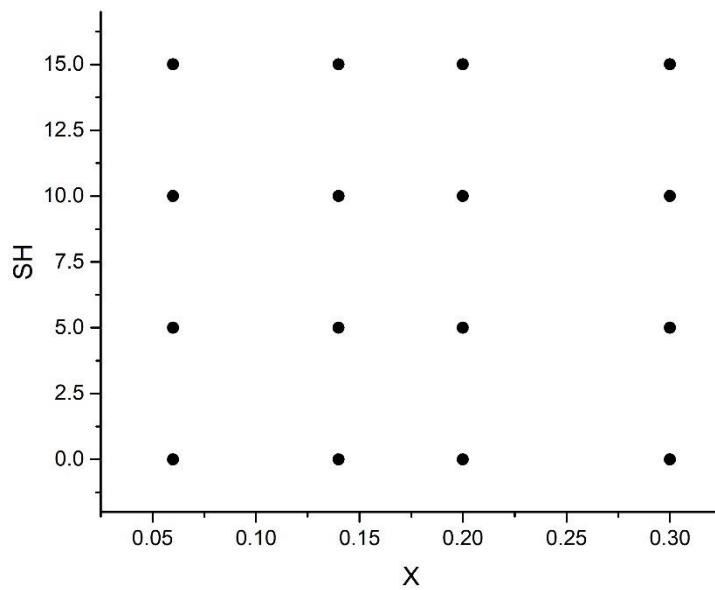
Figure 21. Test matrix for each dTw

Inlet quality was a parameter that was interesting to see its influence during the operation of the heat pumps as flow pattern changes can appear. From own experience, superheat had a negative effect in the performance so the parameter was included in the study. As the heat pumps under study is expected to work for heat recovery applications, the proposed test campaign includes two different water temperature glides, one relatively small and other mother usual for heat recovery applications. So, during the test campaign the following parameters were varied:

- superheat of the evaporation (0K/ 5 K/ 10 K/ 15K)
- inlet quality (0,14/ 0,2/ 0,3)
- temperature difference at the secondary fluid (5 K and 13 K)

The test rig permits to work with and without superheat and different levels of subcooling, giving the choice to change the quality entry. A frequency variable water pump adjusts the water mass flowrate, which will determine the temperature at the outlet of the evaporator.

A thermoresistance is on each side of the evaporator and the water mass flow is measured with a Coriolis mass flow meter. For the pressure on the refrigerant side, three Rosemount sensors are installed. In order to monitor and measure the parameters on the BHPE, all the sensors were connected to a data acquisition system "Agilent 34970A", where all parameters were monitored. Afterwards, stored in a .csv file for data treatment. The relative and absolute accuracy of each device are shown in Table 3.

Table 3. Instrumentation used in the test rig

Magnitude	Model	Relative accuracy	Absolute accuracy
Pressure	P 1151 Smart GP7 Rosemount	0.12 % of Span	0.03
	P 1151 Smart GP8 Rosemount	0.15 % of Span	0.08
	P 3051 TG3 Rosemount	0.14 % of Span	0.04
Temperature	RTD Class 1/10 DIN		0.06
Mass Flow	Coriolis SITRANS F C MASS 2100	0.3 % of Reading	

For the further analysis of maldistribution, the following data were obtained. Some parameters are direct recordings from instrumental devices and others were obtained from them.

Useful data from the refrigerant side:

- Evaporation pressure (P_{evap}): Direct measurement from pressure instrument device at the outlet of the evaporator or inlet of the compressor.

- Evaporation temperature (T_{evap}): Conversion from evaporation pressure.

- Superheat (SH): Expansion valve registered degree of superheat.

- Evaporator inlet quality (x_{in}): This value is obtained differently depending on used working mode of the heat pump. Taking advantage of the p-h map and considering the expansion process isenthalpic for mode C, the inlet quality is obtained by obtaining the enthalpy in point 3 in Figure 22, knowing the degree of SC applied as the condensing pressure is measured. In mode B, pressure is measured in the liquid receiver point 4 in Figure 23 and enthalpy is known and will be equal to the entry at the evaporator.
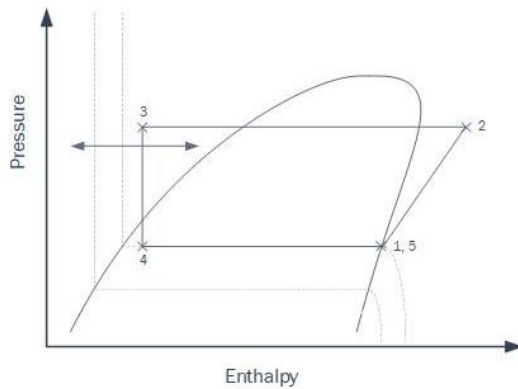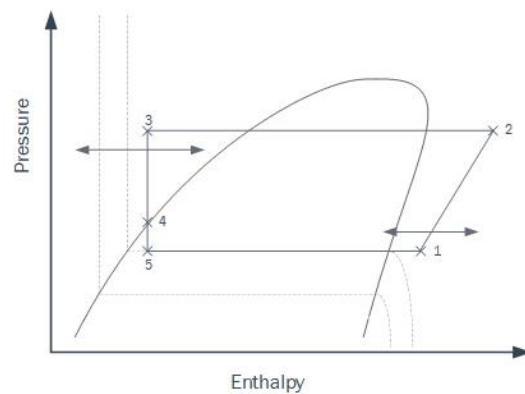
Figure 22. Mode C p-h diagram   **Figure 23. Mode B p-h diagram**

- Evaporator outlet temperature: as the evaporation temperature is known as well as the degree of SH, the temperature at the outlet of the evaporator is calculated as the sum of both.
- Refrigerant mass flow: Refrigerant is not being measured directly by can be obtained by knowing the water mass flow which is measured with a Coriolis measuring device. As the enthalpy at the entry and at the outlet of the evaporator are known, refrigerant mass flow is calculated as follows:

$$Q = m_{ref}\Delta h_{ref} = m_w C_p dT_w \tag{3}$$

$$m_{ref} = \frac{m_w C_p dT_w}{\Delta h_{ref}} \tag{4}$$

Similar calculation has been done in the condenser and the refrigerant mass flow is estimated as the average to decrease the possible error made.

Data obtained from the water side:

- Water mass flow: the water mass flow is calculated directly with a Coriolis measuring device.
- Inlet and outlet water temperature: the installed thermoresistance at the inlet and outlet of the evaporator measure the temperature of the secondary fluid.

To register the refrigerant distribution, the surface of the evaporator is been photographed by IR thermography. It can be seen in Figure 24 that the surface was painted black, to enhance the emissivity factor, which has been photographed and corresponds to the part where the water is entering. The other part is not accessible to take IR pictures. Although this part where refrigerant is entering, the analysis of maldistribution is not affected. Surface temperature is the result of both water and refrigerant being almost the same observed on the other side.
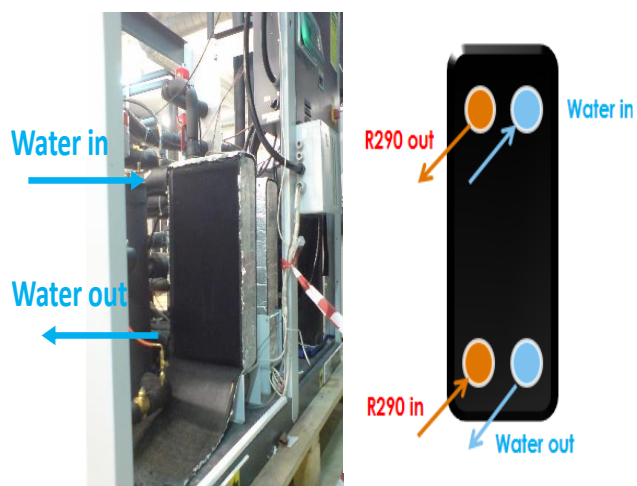
Figure 24. Picture of a frontal view of the evaporator (face used for thermography) and a transversal view with the location of the refrigerant and water inlet/outlet ports

Figure 25. FLIR GF346 Thermography camera

Qualitative thermography tests are performed, this means that we are comparing different point's temperature. The IR camera used is **FLIR GF346** (Figure 1) and its measuring range of was set from -40 to 120ºC. Further details and characteristics of the camera can be found in the annexes.

All thermographies were taken with a water temperature inlet in the evaporator of 20ºC to be comparable with each other and could not be biased by different inlet water temperatures. Although the analysed study is referred to the evaporator, water temperature and outlet at the condenser were set to 20ºC and 60 respectively whenever possible. Once stable conditions were achieved, a 30 min recording of data was performed and the referred thermography is taken for each test.

4.3 IMST-ART SOFTWARE

Within this thesis IMST-ART software is used to predict or compare the heat pump and evaporator performance. It has been introduced in the Justification chapter, but deeper details are given below.

IMST-ART software, developed by the IIE group in UPV, is a dedicated software for modelling, analysis and optimization of refrigeration equipment such as heat pumps systems, freezers or air conditioning units. This software is based on the long experience of the group from its work in design of components and systems and assures a high accuracy on the results by the validation and continuous optimization of the software extracted from real systems.

IMST-ART models allow to evaluate systems, dividing the model in sub-models corresponding to compressor, condenser, evaporator and expansion valve. A Standalone Heat Exchanger module is available and allows the calculation of a heat exchanger independent of the rest of the refrigeration cycle. The heat exchanger is discretized in cells, assuming a one-dimensional flow of refrigerant and

secondary fluid. For each type of the available heat exchangers in the market, IMST-ART selects the most appropriate correlations for heat transfer and pressure drop with local evolution of heat transfer coefficient and friction factor. Introducing the geometrical data of the evaporator or condenser, the global solution employed SEWTLE (Semi-Explicit method for Wall Temperature Linked Equations) can calculate and show the working condition of the heat exchanger or the whole system.

As we are dealing with the maldistribution in the BPHE evaporator, mainly the Standalone module was used. The following information must be introduced about the configuration and size in the definition of the heat exchanger menu in IMST-ART (Figure 26):

- Working mode: heat exchanger working as an evaporator.

- Flow arrangement: Counter-current, refrigerant and secondary fluid are flowing in opposite directions.

- Input/output pressure losses: Data referred to the header and the distributor devices must be indicated. Normally, this is confidential and secret manufacturer information, so nothing could be filled in this part.

- Total number of plates: 120. Half of the plates are dedicated to the refrigerant and the other for the secondary fluid.

- Plate material: steel, as it is a brazed plate heat exchanger.

- General geometrical data: To fill this data, the scheme of the evaporator manufacturer was used and shown in figure 27:
    o HPCD: Horizontal Port Centre Distance, the horizontal distance between the centres of the ports: 50 mm
    o VPCD: Vertical Port Centre Distance, the vertical distance between the centres of the ports: 466 mm
    o Port Diameter: Inner port diameter: 16 mm

    o Plate Pitch: the separation distance between two plates and the plate thickness. The thickness is normally not indicated by the manufacturer but can be considered around 0,35 mm. The plate separation has been calculated as the division of the width (287 mm) by the number of plates (120).
    o Channel type: the type of angle in the channel corrugation, the higher the angle, the higher the heat transfer and the pressure drop: Medium (M)
    o Area Enhancement factor: recommended by ASHRAE: 1.17.

The enhancement factors are multiplires that affect heat transfer coefficient, or the pressure drop. These are used to adjusted IMST-ART calculations with experimental results. In this work and explained in CHAPTER 5. Obtainted Results and Analysis, a minor value for the enhancement factor for heat transfer has been used to simulate the effect of maldistribution.
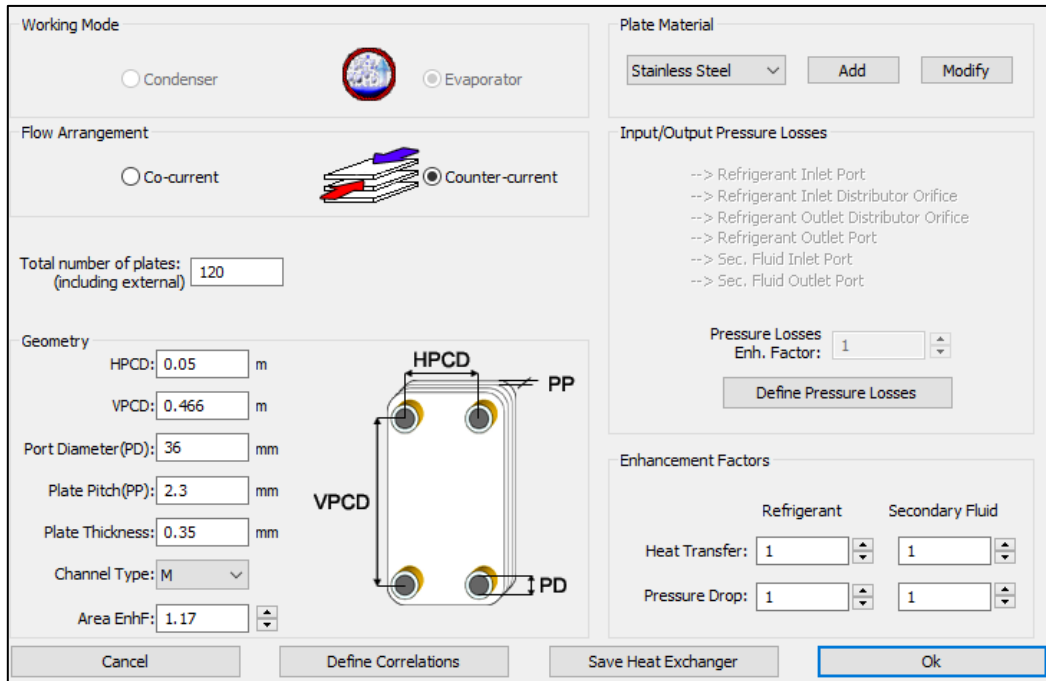
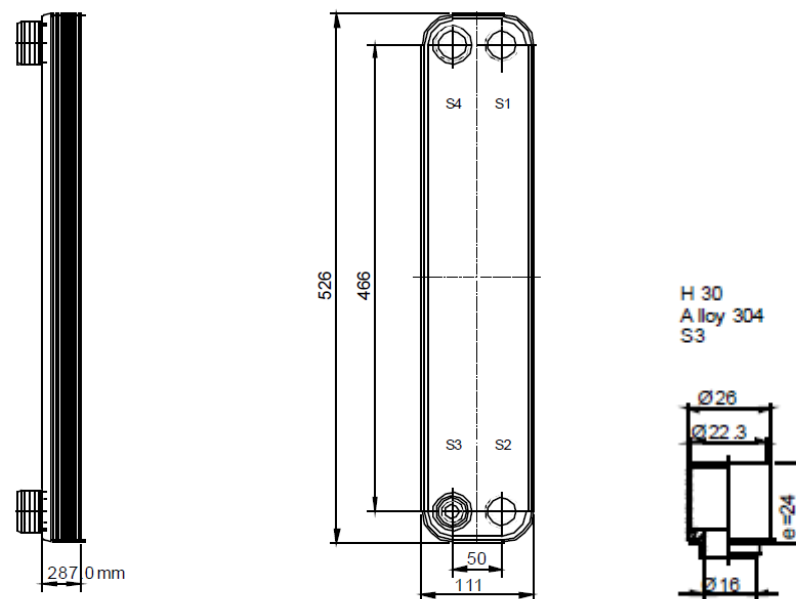**Figure 26. Definition of the heat exchanger in IMST-ART**

Figure 27. Dimensions of the evaporator. Data from manufacturer

Figure 28. Main menu of the Standalone module of IMST-ART.

Once the geometrical data of the heat exchanger is introduced, in the main menu (Figure 28) of the Standalone module, further information must be introduced referred to the refrigerant and the secondary fluid. As water and propane are running the heat pump, this will be the selected fluid. Information about mass flow rates, superheat, inlet quality, Inlet and outlet temperatures will be selected from the results of the test campaign.

3.4 THERMOCAM RESEARCHER PRO 2.10

ThermoCam is a dedicated software for infrared pictures study developed by IR-cameras manufacturer FLIR. It is able to study real-time infrared recordings and static pictures.

For this thesis, it easy pictures data treatment and its built-in temperature measurement is used. It is capable to show temperature information of spots, lines and areas: maximum temperature, minimum, average…

Its intuitive interface allows non-expert people to manipulate thermographies and make simple temperature analysis. Understand what the information given by themography pictures is essential for this work.

Given the following example in Figure 29, a line can be drawn in the thermography and the software is able to show line temperature profiles and histogram charts. The temperature profile will be the most useful in order to compare simulation results with the obtained experimental observations.
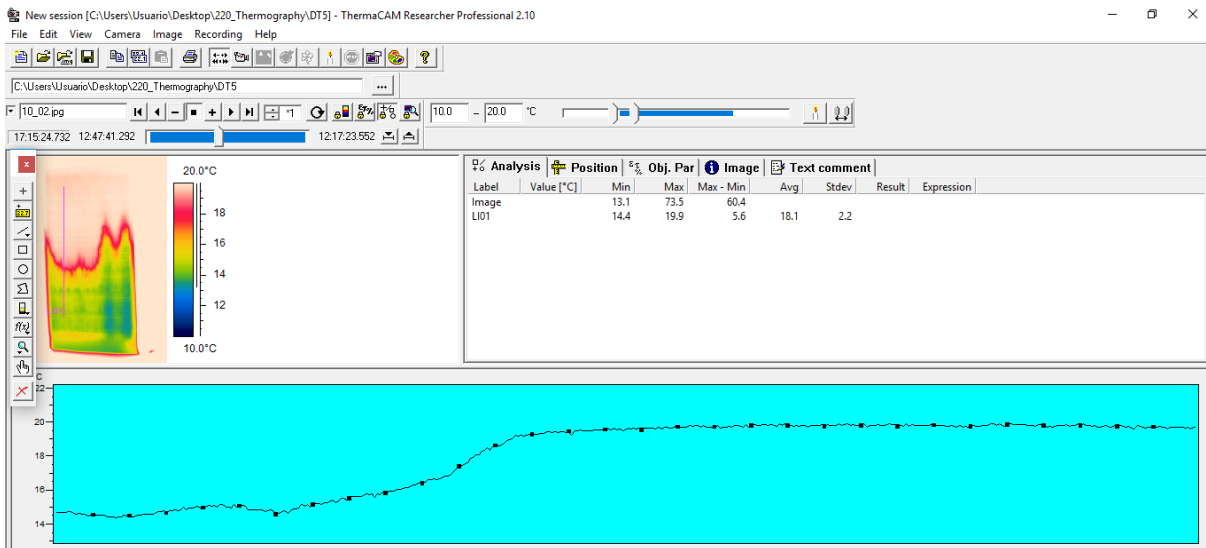
Figure 29. ThermoCam temperature profile analysis.

Although the wall temperature is measured by the thermographic camera, it is stated that we are observing the heat transfer exchanged by the fluids. It can be seen that almost a constant temperature of 20ºC is observed in the upper part of the evaporator, water is not transferring heat as a superheat zone is present; heat transfer coefficient in single-phase is much lower than in two-phase flow. Then, a sudden drop of the temperature is found, refrigerant two-phase flow appears and heat transfer increases, thus water temperature decrease as well as wall temperature.

CHAPTER 5. OBTAINTED RESULTS AND ANALYSIS

In this chapter the results of the experimental campaign are compared with simulation software in order to measure the effect of the maldistribution in the evaporation temperature and diminish the effect of thermodynamics (superheat and inlet quality), a software is used to obtain theoretical evaporation temperatures.

Another aspect is observed here is what occurred when almost liquid was flowing. From literature review, a possible solution to avoid maldistribution is liquid flow at the entry of the evaporator, like a flooded evaporator. Trials out of the main experimental campaign with different degree of SH and low inlet qualities were performed.

5.1 EXPERIMENTAL RESULTS

The next Table 4 shows the corresponding IR thermography for a water temperature difference of 5 K. They are given in tables in the corresponding order of superheats. The minimum temperature of the scale is set to 10 ºC and the maximum to 20 ºC. This means that temperatures below and around 10 ºC are shown in a dark-blue colour whereas bright colours are for intermediate temperature. Red are for temperatures near 20 ºC and white for temperatures above.

The next Table 5 shows the corresponding IR thermographies for a water temperature difference of 13 K. They are given in tables in the corresponding order of superheats. The minimum temperature of the scale is set to -5ºC and the maximum to 15ºC. If the previous scale were used, no bright colours were distinguished, only a dark-blue frame.

The experimental results of each test are presented below the afterwards mentioned tables. They are not ordered like the thermography pictures. They are listed from the lowest superheat value to the highest, for the case of mode B, as well as for the inlet quality. They are separated in two tables, one which corresponds to the Mode B working mode in Table 6, this is with a certain degree of superheat and the other the data referring to mode C in Table 7.

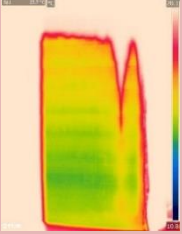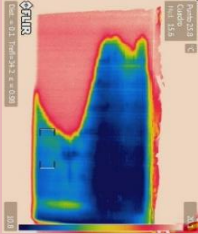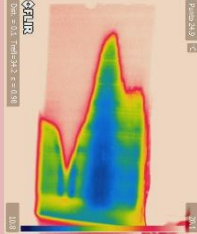**Table 4. Thermographies for dT$_{water}$= 5 K with variation of inlet quality and superheat**
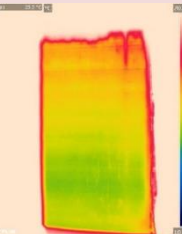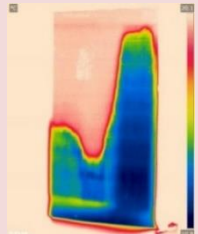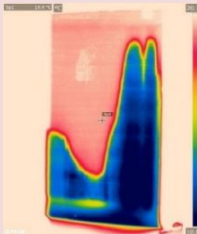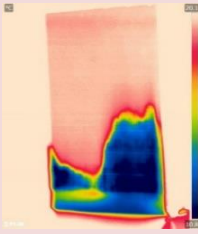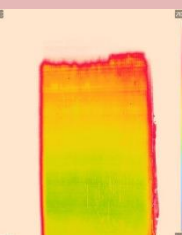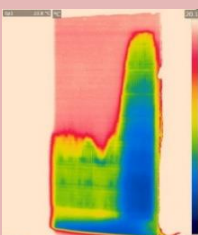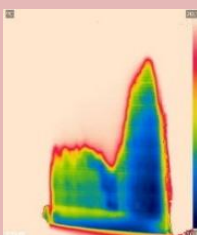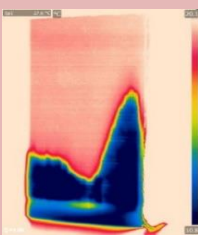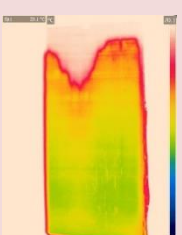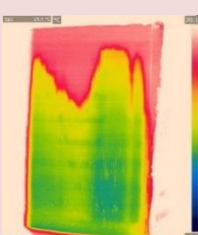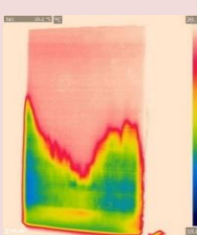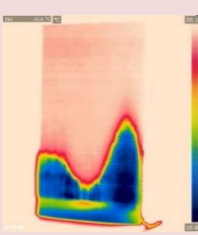
dT$_w$ 5K	SH= 0 K	SH= 5K	SH= 10 K	SH= 15 K
x=0.06	T$_{evap}$= 12.34 ºC dTw= 5.26 x=0.053	T$_{evap}$= 10.34 ºC dTw= 4.58 x=0.078	T$_{evap}$= 9.00 ºc dTw= 5.17 x=0.085	T$_{evap}$= 4.61 ºC dTw= 5.3 x=0.068
x=0.14	T$_{evap}$= 12.81 ºC dTw= 5.22 x=0.142	T$_{evap}$=8.37ºC dTw= 5.4 x=0.141	Tevap=7.39ºC dTw = 5.3 x=0.141	Tevap=4.61ºC dTw = 4.9 x=0.142
x=0.2	T$_{evap}$= 13.21 ºC dTw= 4.85 x=0.199	T$_{evap}$=10.01ºC DTw = 4.3 x=0.191	T$_{evap}$=8.42ºC dTw = 4.9 x=0.185	T$_{evap}$=4.8ºC dTw = 5.1 x=0.208
x= 0.3	T$_{evap}$= 13.34 ºC dTw= 4.859 x=0.305	T$_{evap}$=12.71ºC dTw= 4.6 x=0.322	T$_{evap}$=9.50ºC dTw= 4.6 x=0.289	T$_{evap}$=4.92ºC dTw= 4.8 x=0.303

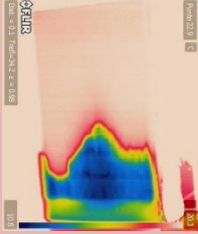**Table 5. Thermographies for dT$_{water}$= 13 K with variation of inlet quality and superheat**
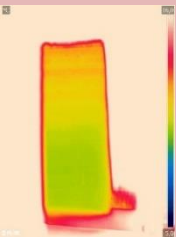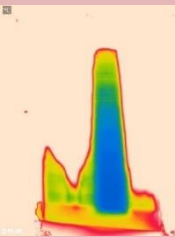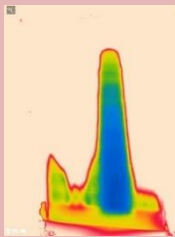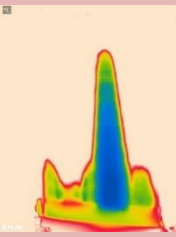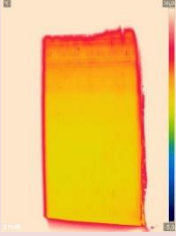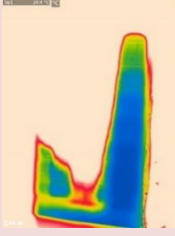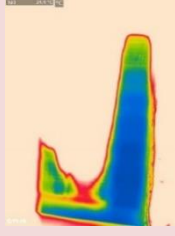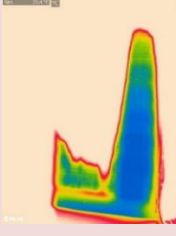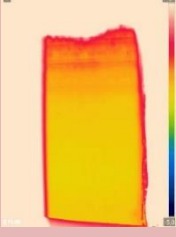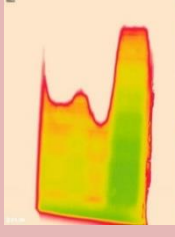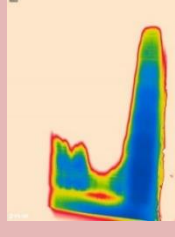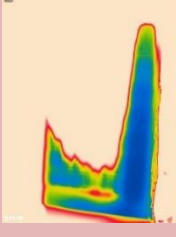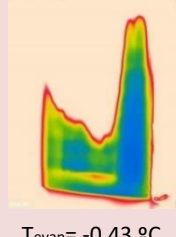
dT$_w$ 13K	SH= 0 K	SH= 5K	SH= 10 K	SH= 15 K
x=0.06	T$_{evap}$= 4.05 ºC dTw= 12.9 x=0.042	T$_{evap}$= -1.02 ºC dTw= 13.2 x=0.064	T$_{evap}$= -1.8 ºC dTw= 12.9 x=0.069	T$_{evap}$= -1.88 ºC dTw= 12.9 x=0.072
x=0.14	T$_{evap}$=5.9 ºC dTw= 13.04 x=0.142	T$_{evap}$= -2.02 ºC dTw= 13.1 x=0.139	T$_{evap}$= -2.46 ºC dTw= 13 x=0.139	T$_{evap}$= -1.88 ºC dTw= 13 x=0.141
x=0.2	T$_{evap}$= 6.14ºC dTw= 12.88 x=0.198	T$_{evap}$= -1.43 ºC dTw= 12.7 x=0.209	T$_{evap}$= -2.08 ºC dTw= 12.5 x=0.215	T$_{evap}$= -2.31 ºC dTw= 12.77 x=0.199
x= 0.3	T$_{evap}$= 6.02 ºC dTw= 13 x=0.295	T$_{evap}$= 4.8 ºC dTw= 13.1 x=0.291	T$_{evap}$= 3.67ºC dTw= 13.2 x=0.304	T$_{evap}$= -0.43 ºC dTw= 13.1 x=0.268

Table 6. Experimental results for mode B.

	nº	Water Evaporator					Refrigerant Evaporator							
		T_in	T_out	dTw	mass flow	capacity	quality	mass flow	mass flow	mass flux	T_evap	T_out	SH	COPc
		°C	°C	K	kg/s	kW	[-]	kg/s	kg/h	kg/m^2 S	°C	°C	°C	[-]
	1	19.96	15.38	4.58	1.94	37.23	0.08	0.11	385.20	532.34	10.34	16.64	6.29	4.83
	2	20.01	14.57	5.44	1.43	32.45	0.14	0.10	360.00	497.51	8.38	13.70	5.33	3.88
	3	19.89	15.59	4.30	1.80	32.36	0.19	0.11	381.60	527.36	10.01	15.03	5.02	3.88
	4	19.76	15.12	4.64	1.51	29.37	0.32	0.12	414.00	572.14	12.71	17.41	4.70	3.59
	5	19.97	14.80	5.17	1.65	35.77	0.09	0.10	363.60	502.49	9.00	19.12	10.12	4.94
	6	20.01	14.70	5.31	1.43	31.71	0.14	0.10	342.00	472.64	7.39	18.26	10.87	3.84
	7	20.01	14.82	5.19	1.48	32.19	0.20	0.10	370.80	512.44	9.79	19.48	9.69	3.92
	8	19.97	15.40	4.58	1.52	29.04	0.29	0.10	370.80	512.44	9.51	19.60	10.09	3.60
	9	20.03	14.73	5.31	1.48	32.90	0.07	0.09	316.80	437.81	4.61	19.83	15.22	5.19
MODE B	10	19.98	15.04	4.94	1.43	29.52	0.14	0.09	306.00	422.89	4.61	19.57	14.96	3.60
	11	20.01	14.93	5.09	1.30	27.60	0.21	0.09	309.60	427.86	4.80	19.60	14.80	3.45
	12	19.91	15.11	4.80	1.29	25.94	0.30	0.09	320.40	442.79	4.92	19.58	14.66	3.28
	13	19.92	6.69	13.23	0.48	26.83	0.06	0.08	294.39	406.84	-0.99	5.09	6.08	2.82
	14	19.95	7.04	12.91	0.48	26.23	0.07	0.08	280.29	387.35	-1.82	8.80	10.62	2.90
	15	19.96	7.05	12.91	0.48	26.23	0.07	0.08	273.94	378.59	-1.90	13.35	15.24	2.97
	16	19.93	6.83	13.11	0.46	24.97	0.14	0.07	262.80	363.18	-2.02	3.08	5.10	3.71
	17	19.92	6.91	13.01	0.46	24.79	0.14	0.07	255.60	353.23	-2.46	7.72	10.17	3.75
	18	19.90	6.89	13.01	0.47	25.67	0.14	0.07	259.20	358.21	-1.88	13.27	15.14	4.41
	19	19.91	7.14	12.77	0.44	23.27	0.20	0.07	252.00	348.26	-2.31	12.84	15.15	3.30
	20	19.97	7.22	12.75	0.44	23.25	0.21	0.07	266.40	368.16	-1.73	4.00	5.73	3.22
	21	19.95	7.46	12.50	0.44	22.80	0.22	0.07	259.20	358.21	-2.46	7.50	9.95	3.22
	22	19.93	6.82	13.11	0.41	22.50	0.27	0.07	266.40	368.16	-0.46	14.52	14.98	2.90
	23	19.91	6.77	13.14	0.46	25.16	0.29	0.09	327.60	452.74	4.80	10.22	5.42	3.62
	24	19.97	6.79	13.18	0.44	24.13	0.30	0.09	309.60	427.86	3.67	14.14	10.47	3.18

Table 7. Experimental results for mode C.

	nº	Water Evaporator					Refrigerant Evaporator							
		T_in	T_out	dT_w	mass flow	capacity	quality	mass flow	mass flow	mass flux	T_evap	T_out	SH	COPc
		°C	°C	K	kg/s	kW	[-]	kg/s	kg/h	kg/m^2 S	°C	°C	°C	[-]
MODE C	25	20.05	14.79	5.26	1.84	40.59	0.05	0.12	429.54	593.61	12.36	12.93	0.56	4.71
	26	20.08	14.86	5.22	1.64	35.75	0.14	0.12	425.53	588.08	12.82	13.26	0.43	4.14
	27	20.03	15.18	4.85	1.61	32.76	0.20	0.12	423.45	585.20	13.21	13.64	0.43	3.78
	28	20.06	15.20	4.86	1.27	25.90	0.31	0.11	397.65	549.54	13.36	13.75	0.39	3.04
	29	20.02	7.12	12.90	0.61	32.74	0.04	0.09	335.28	463.36	4.04	4.77	0.73	3.56
	30	19.98	6.94	13.04	0.54	29.28	0.14	0.10	343.85	475.19	5.90	6.52	0.61	3.47
	31	20.13	7.25	12.88	0.49	26.37	0.20	0.09	339.44	469.09	6.19	6.59	0.40	3.12
	32	20.04	7.03	13.01	0.36	19.76	0.30	0.08	302.43	417.95	6.02	6.44	0.42	2.52

The following aspects can be clearly stated from the thermography pictures presented in Table 4 and Table 5:

- The two-phase flow region can be identified by a sharp red line.
- For operation with superheat points, the two-phase flow region is not even distributed, indicating a maldistribution of the refrigerant mass flow. The right or the central part of the heat exchanger is shown to be occupied by two-phase flow. This indicates a higher mass flow rate in this part of the heat exchanger.
- The inlet quality influences the distribution. A higher inlet quality leads to a more even distribution of the two-phase flow region. However, higher inlet quality seems to not improve distribution for dT_{water} = 13 K.
- For higher superheats the two-phase flow area is smaller than for lower superheats, the same superheat can be assumed for all channels.
- For lower superheat and inlet qualities the two-phase flow of the right part of the heat exchanger occupies the whole length of the channel. There the required superheat is probably not reached.
- Optimum refrigerant distribution is achieved when no superheat is performed although vapor is entering. As outlined in [29], this were only possible when no vapor was entering. However, for low inlet quality, refrigerant distribution seems to not improve.

5.2 EVAPORATION TEMPERATURE

As explained in the justification chapter, the obtained evaporation temperature during the operation of the heat pump was far from the expected. Therefore, a deeper analysis and evaluation of the evaporation temperature is done.
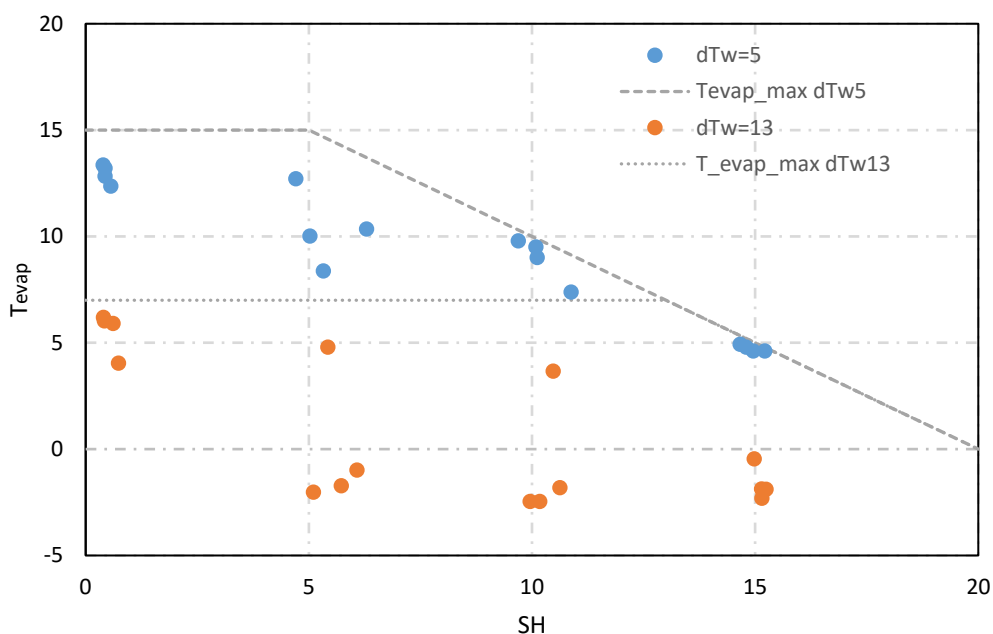
Figure 30. Evaporation temperature from the point of view of the degree of SH

In Figure 30, evaporation temperature from the test campaign results are plotted. In a dotted grey line, the maximum evaporation temperature is shown. In the x-axis, SH is placed whereas in the y-axis the

evaporation temperature is assigned. It can be clearly observed that the highest evaporation temperature is obtained for the cases for dTw=5 and zero SH. Evaporation temperature decreases to fit the fixed dTw. However, for high SH and dTw=5, the evaporation temperature corresponds to the maximum and the evaporator is working at its maximum performance, evaporation temperature decreases as much to provide the set degree of superheat. However, for the cases SH=dTw or SH<dTw evaporation temperature suffers a degradation in the evaporation temperature and therefore, in the performance of the evaporator.

Similar as in the figure shown begore, in Figure 31 in the x-axis, the water outlet temperature is plotted. The evaporation temperature that are closer to the grey line are closer to the water outlet temperature. Here are the tests that are with no SH and some of with a degree of SH that is lower that the temperature drop. As stated before, having a value for dTw higher than the level of SH leads to a drastically decrease in evaporation temperature.
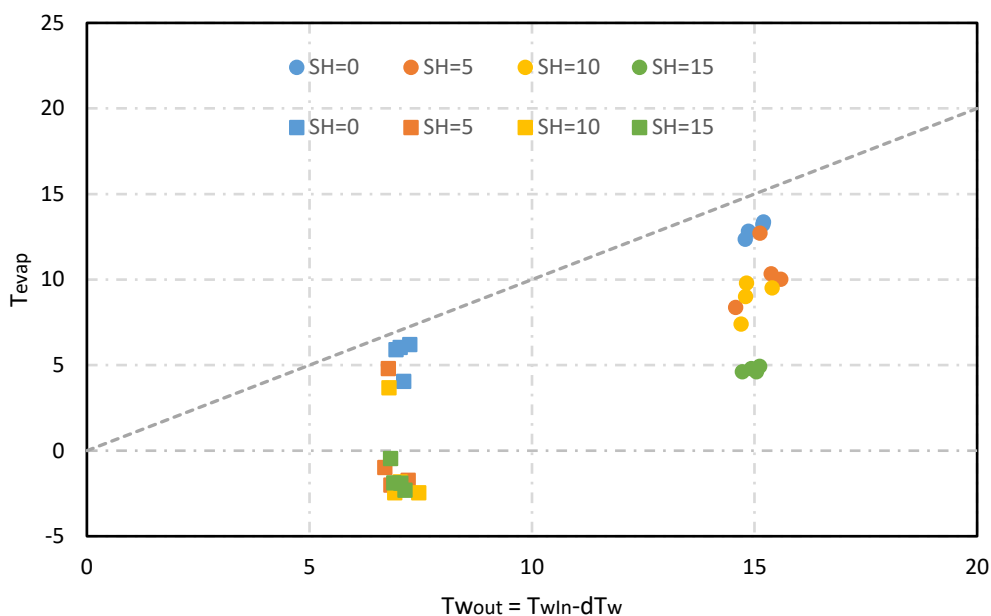
Figure 31. Evaporation temperature from the point of view of the outlet water temperature

From data of the experimental campaign, evaporation temperature is plotted in function of the SH and the water temperature drop dTw by applying a spline interpolation. In this Figure 32 it can be clearly seen how the saturation temperature is influenced by the working conditions of the heat pump: best working performance is obtained by working with no SH. A high degree of SH has inherited a high evaporation temperature drop likewise for a high temperature glide.
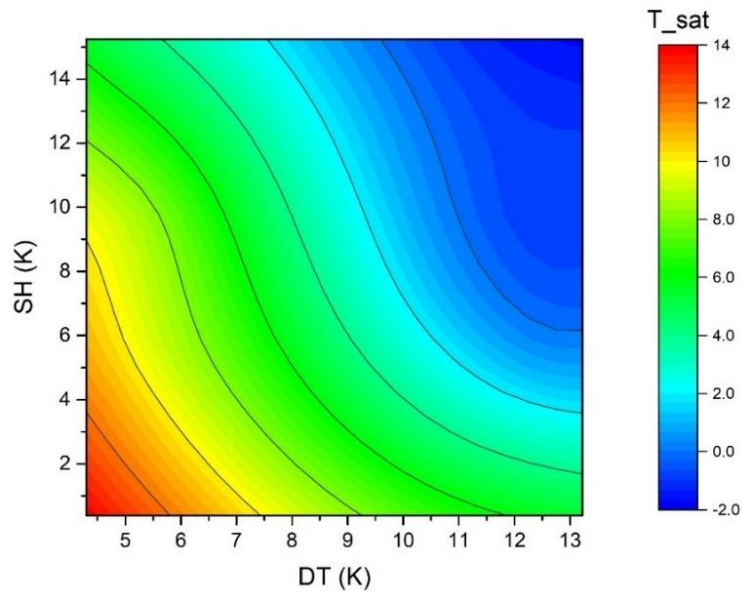
Figure 32. Evaporation temperature in function of the SH and dTw of the experimental campaign

One conclusion would be that the temperature drop on the secondary fluid should not be higher than the amount of the degree of SH. A higher water temperature drop has inherited a decrease in the performance by a noticeable decrease in the evaporation temperature. However, a too low secondary fluid temperature glide requires an excessive consumption of the pumps leading to a COP degradation. It is therefore recommendable that the secondary fluid flow rate and expansion valve conditions should be selected to give such a degree of SH that is lower than the temperature drop of the secondary fluid. However, for heat recovery application where the water temperature drops attempt to be high (>10 K), the use of superheat might be interesting but from this first analysis not recommended.

5.2 COMPARISON WITH SIMULATION SOFTWARE

The results of the experimental campaign are compared with IMST-ART simulation tool. IMST-ART allows to the calculation of a heat exchanger independent of a vapour compression cycle working as condenser or evaporator. The interest of this comparison is that commercial software supposes a homogeneous distribution of refrigerant and secondary fluid. The parameter of interest is the evaporation temperature. This parameter can be comparable to COP of a heat pump system. The pressure difference between the low-pressure side (evaporator) and the high-pressure side (condenser) should be as small as possible to reduce energy consumption in the compressor. The higher the evaporation temperature, the higher the refrigerant density. Therefore, for each stroke the compressor can transport more refrigerant. Lower consumption and higher capacity will increase the total system efficiency.

The main information from the test campaigns are introduced in the software:

- Secundary fluid: Fluid, Inlet temperature and outlet temperature
- Refrigerant: Fluid, mass flow rate, inlet quality and SH

Geometrical data has been filled as explained in 4.3 IMST-ARt Software.

The obtained results from software are compared with the experimental results and plotted in two Figure 33 and Figure 34 for the different secondary fluid temperature glide, 5 and 13 K. Both figures have plotted in a dotted grey line the maximum saturation temperature given by equation (1).

Evaporation temperature calculated with software are in the most part of the cases close to the maximum evaporation temperature. For low temperature glides (Figure 33), inlet quality seems to have no effect on evaporation temperature being for same values of SH, almost the same saturation temperature. Contrarily for high temperature glides, lower evaporation temperatures are obtained for low inlet quality (x=0.07). However, evaporation temperature from experimental campaign show for low inlet quality rather higher temperatures than for other qualities. Inlet quality of x=0.3 have always higher saturation temperatures.

For dTw=5 and high SH, evaporation temperature matches with IMST-ART results and are almost at the maximum permissible thermodynamically.
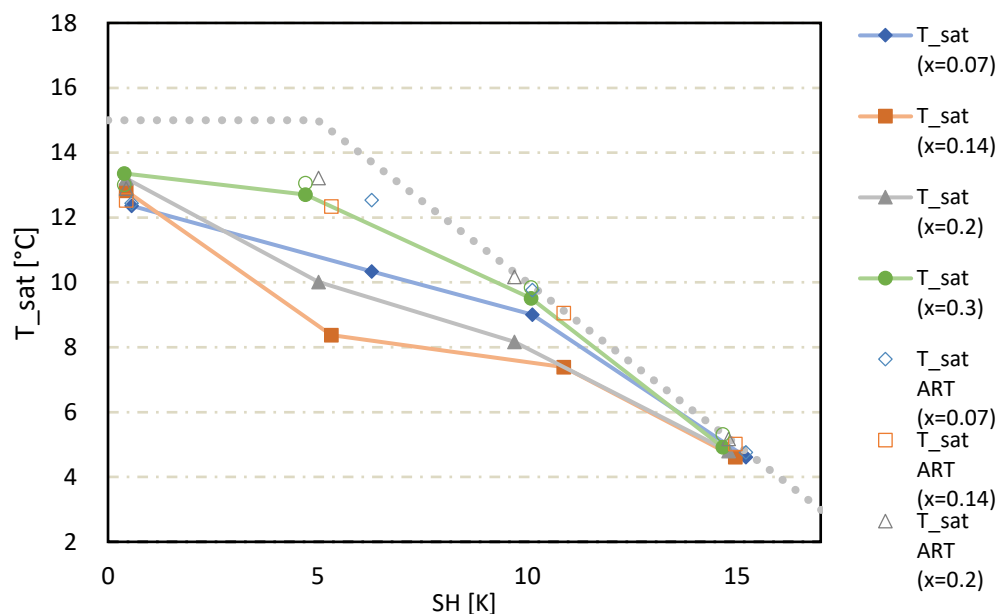
Figure 33. Evaporation temperature comparison for dTw=5K

Similar observations are made for dTw=13K. As seen in Figure 34, evaporation temperature for high dTw suffer a high decrease and are the most part of the cases negative. Inlet quality of x=0.3 have always higher saturation temperature.
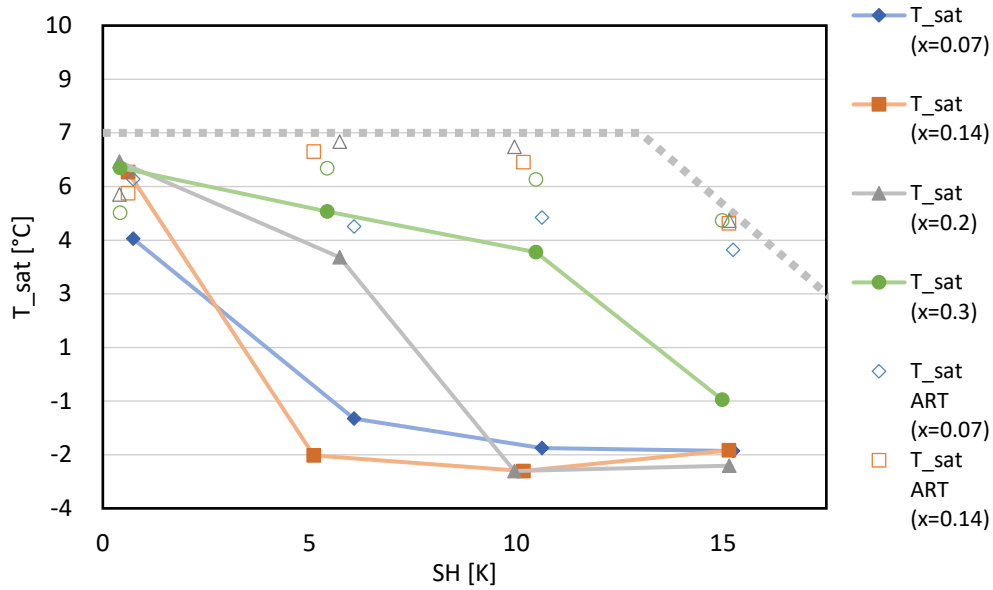
Figure 34. Evaporation temperature for dTw=13K

For a further analysis, evaporation temperature is evaluated within inlet quality and SH. Starting for dtw=5, shown in Figure 35 higher evaporation temperature values are obtained with low or zero SH and decreases with SH. At first sight inlet quality has affect the evaporation temperature for low SH, achieving higher evaporation temperature for high qualities, but gets for high SH independent of quality. A sudden decrease of evaporation temperature is observed in (SH=5, x=0.14). In the Figure 36 below, the absolute temperature difference between IMST-ART and the experimental results is shown. The mentioned decrease in evaporation temperature is the noticeable disagreement with simulation software. Otherwise, prediction with software is for this temperature glide at the evaporator rather accurate.
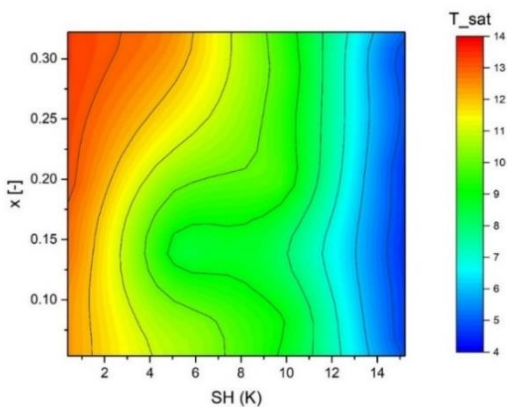
Figure 35. Saturation temperature for dT$_w$= 5   **Figure 36. Absolute T$_{sat}$ difference for dT$_w$= 5**
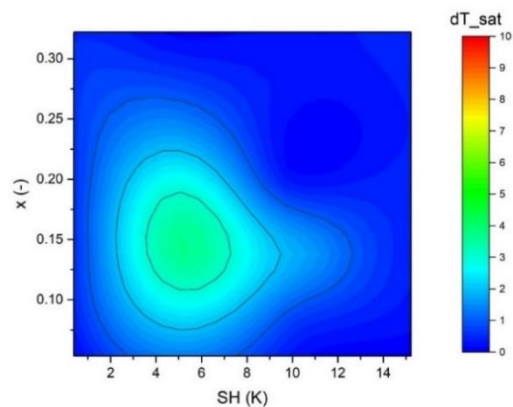
Same plot for temperature glide of 13 K in Figure 37 has been done. Similar results are obtained: for zero SH higher evaporation temperatures are achieved and is decreasing with SH. However, for high inlet qualities more elevated temperatures are reached for a given SH. Absolute differences with IMST-ART follow a similar trend: the higher the evaporation temperature, the smaller the difference.
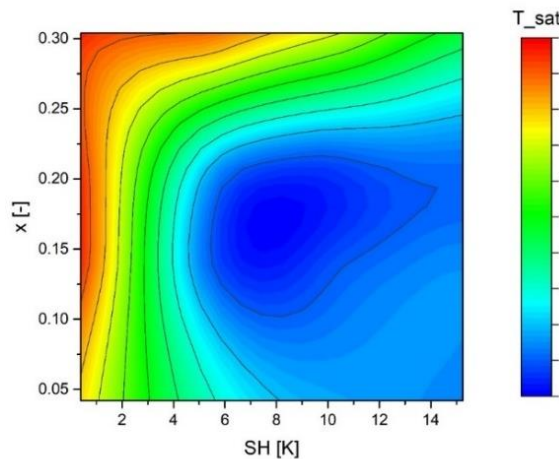
Figure 37. Saturation temperature for dT$_w$= 13   **Figure 38. Absolute T$_{sat}$ difference for dT$_w$= 13**
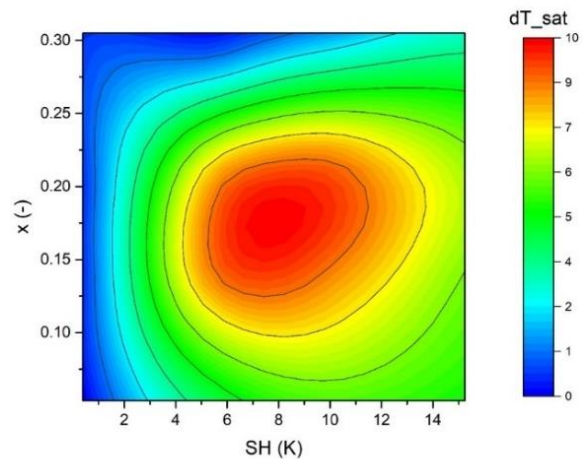
From this analysis a clear effect of dTw on maldistribution is observed. Evaporation temperature is for low dTw more related with SH as for high dTw. The disagreement with simulation software which assumes a homogenous flow of refrigerant is more noticeable for high dTw. Furthermore, a better distribution for high inlet quality (x=0.3) is observed. It may suggest that the own distributor of the evaporator is designed for high inlet qualities, where vapor maldistribution is more severe.

5.4 TWO EVAPORATOR MODEL

Most of the thermographic pictures show an uneven temperature distribution: one that can be called superheated part and another with a higher two-phase flow. The superheated part is mostly smaller and observed on the left part of the evaporator. However, this is not observed in all the taken thermographies.

As a proposed hypothesis, the heat exchanger can be divided in two parts: subexchanger 1, with high SH, and subexchanger 2 with low/zero SH. From literature, it has been observed and stated that in the most cases vapor is entering the first plates. As no SH is observed in the right part, to achieve the measured SH, on the left part a much higher degree of SH must be applied. Therefore, it is expected lower refrigerant mass flow in the part 1 and higher refrigerant mass flow in part 2. Figure 39 resumes the proposed idea.
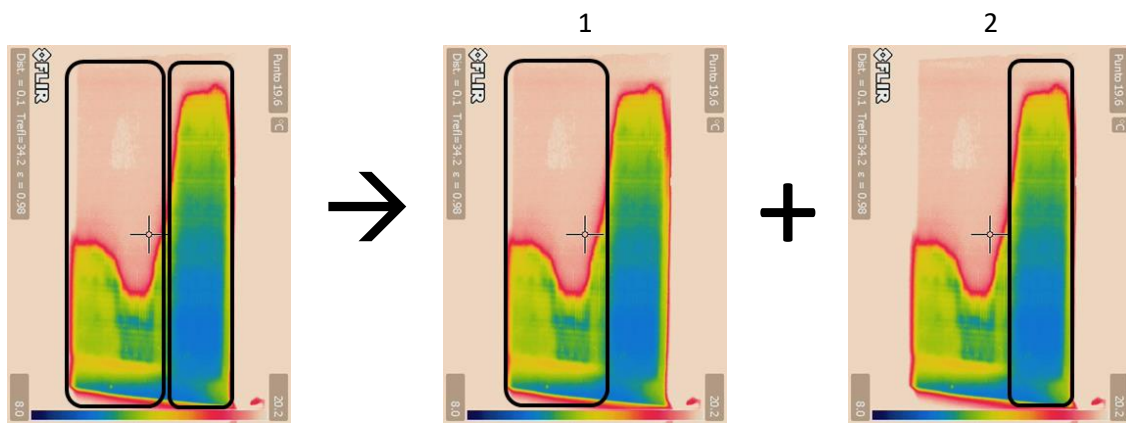
Figure 39. Evaporator separation into two subexchanger that have different conditions

In order to quantify maldistribution, parameter beta is defined as:

$$\beta = \frac{m_1}{m_{ref}} \qquad (5)$$

Similar to beta coefficient, alpha is defined as:

$$\alpha = \frac{m_{w1}}{m_w} \qquad (6)$$

In means of validation of the hypothesis, the experimental data and the thermographic pictures of the tests were used. Divding the evaporator in two parts the following requirements must be fulfiled:

- The sum of both refrigerant flows must be equal to total:

$$m_{ref} = \beta m_{ref} + (1 - \beta)m_{ref} \qquad (7)$$

Or,

$$m_{ref} = m_1 + m_2 \qquad (8)$$

- Inlet quality of both subexchangers must fullfill the corresponding vapor mass balance. Similar to the expression above:

$$x_i = \beta\, x_1 + (1 - \beta)x_2 \qquad (9)$$

- The mixed outlet water temperature of each subexchanger should be equal to the outlet water temperature:

$$T_{w\,out} = \alpha\,T_{w\,out_1} + (1-\alpha)\,T_{w\,out_2}$$

(10)

- Pressure drop throughout the two subexchanger must be equal:

$$PD_1 = PD_2$$

(11)

- Both subexchanger must have the same evaporation temperature:

$$T_{evap_1} = T_{evap_2}$$

(12)

- Both SH in the subexchangers must be proportional to the measured SH in the test, thus:

$$SH = \beta\,SH_1 + (1-\beta)\,SH_2$$

(13)

- The number of plates of both subexchanger must be equal to the total number of plates of the original heat exchanger:

$$N = N_1 + N_2$$

(114)

The scheme of of two subexchangers is represented in the following Figure 40. The before mentioned parameters are included for the better understanding:
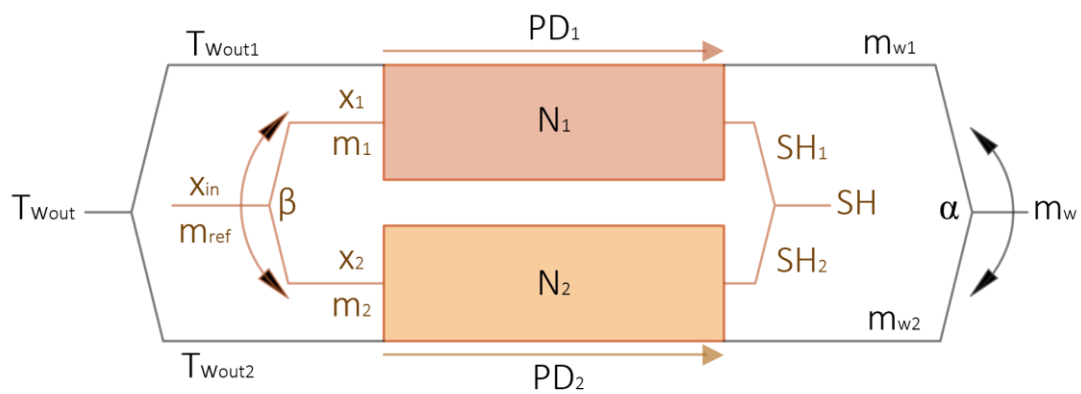
Figure 40. Scheme of the two evaporator model. All the related parameters are exposed.

The two evaporator model can be studied using the commercial software IMST-ART (IMST-ART v.4.00) [48].

Dividing the evaporator in two evaporators, and imposing the inlet conditions, these must accomplish the requirements stated. The must behave like the original evaporator. The Inlet conditions are the following:

- β: it states how the refrigerant is distributed within each subexchanger
  - m_1: refrigerant flow through subexchanger 1
  - m_2: refrigerant flow through subexchanger 2
- α: it states how the water is distributed within each subexchanger. The total water mass flow is known. This is highly related with the number of plates of each subexchanger.
- x_1: the quality of the first subexchanger
- x_2: the quality of the second subexchanger
- T_{evap}: evaporation temperature is the same for both. Directly taken from the experimental results.

However, there is need for assumptions: none of these inlet conditions are known but are related with each other. It is observed in the cases where "two evaporators" are observed, on the right part almost no SH can be supposed thus, more liquid is entering and from literature stated that almost only liquid is flowing. Therefore, imposing values for, β, m_2 ($m_2 > m_1$) and x_2 ($x_2 < x_1$) the values of the subexchanger 1 are directly related. The total water mass flow is known. It has been supposed that water suffers no maldistribution so a value of $\alpha = 0.5$ is stated. The number of plates for each heat exchanger varied.

The reader should be aware of there exists, at least, one solution for the two evaporator model, the obvious and elemental solution: when the same inlet quality and mass flow is flowing through each subexchanger with the same evaporation temperature, both subexchanger conditions are equal and fulfil the imposed requirements. But this mathematical solution is correct but do not correspond with any taken thermography.

Table 8. Two evaporator solution for the case #6

Case #6	SH	dT_w	x_i	Mass flow kg/h	
	10	5	0.14	360	
	SH_1	SH_2	x_1	x_2	β
	12.6	12.4	0.2	0.09	0.41

A full developed parametric study has been developed to obtain similar results as the observed in thermography. It was possible to reproduce some more or less the cases but in others was difficult to achieve. The main problem was that pressure drop and superheat criteria were difficult to accomplish. This suggests that an additional pressure drop of the distribution orifice or the header is not being

taken into account. But to continue in this direction a deeper knowledge on geometrical aspects of the plates and pressure drop within the heat exchanger would be needed.

One of the best examples is being exposed below and its parameters present in Table 8. Although the stablished criteria were not completely fulfilled, the temperature profile of two evaporator model used in IMST-ART agreed with the obtained in the thermography. In the IMST-ART software taken snapshots Figure 41 and Figure 42, the red line corresponds to the refrigerant, the green line to the secondary fluid and blue to the wall temperature. Using commercial software ThermoCam, the referred thermography was selected, and two lines were drawn in the two different zones to obtain the temperature profile of the picture: the blue line corresponds to the superheated zone while the red profile to the two-phase zone.

It can be clearly seen that the temperature line extracted from ThermoCam Figure 43 follows the wall temperature profile that is calculated by IMST-ART. On the one hand, for the first subexchanger, wall temperature is 20ºC for almost the whole length of the evaporator but when encountered with the two-phase flow, the temperature drops. On the other hand, for the second subexchanger wall temperature is invariant during the first upper part of the heat exchanger at 20ºC, sudden drop occurs and falls gradually.
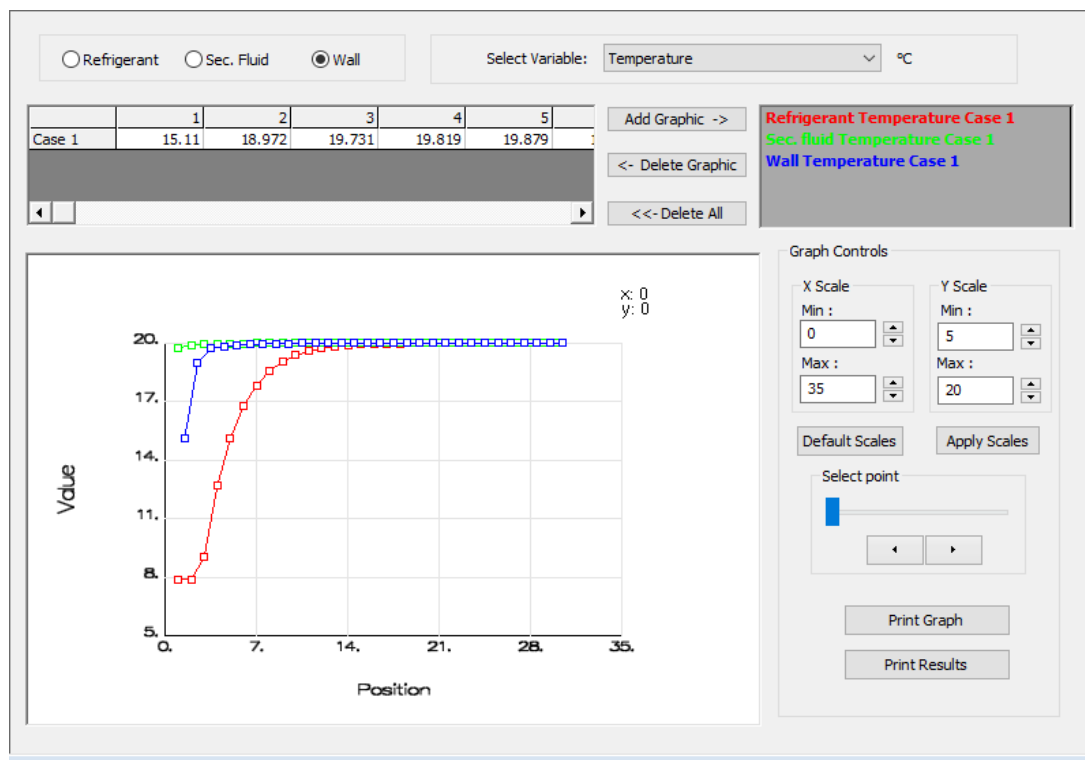
Figure 41. Temperature profile of the subexchanger 1
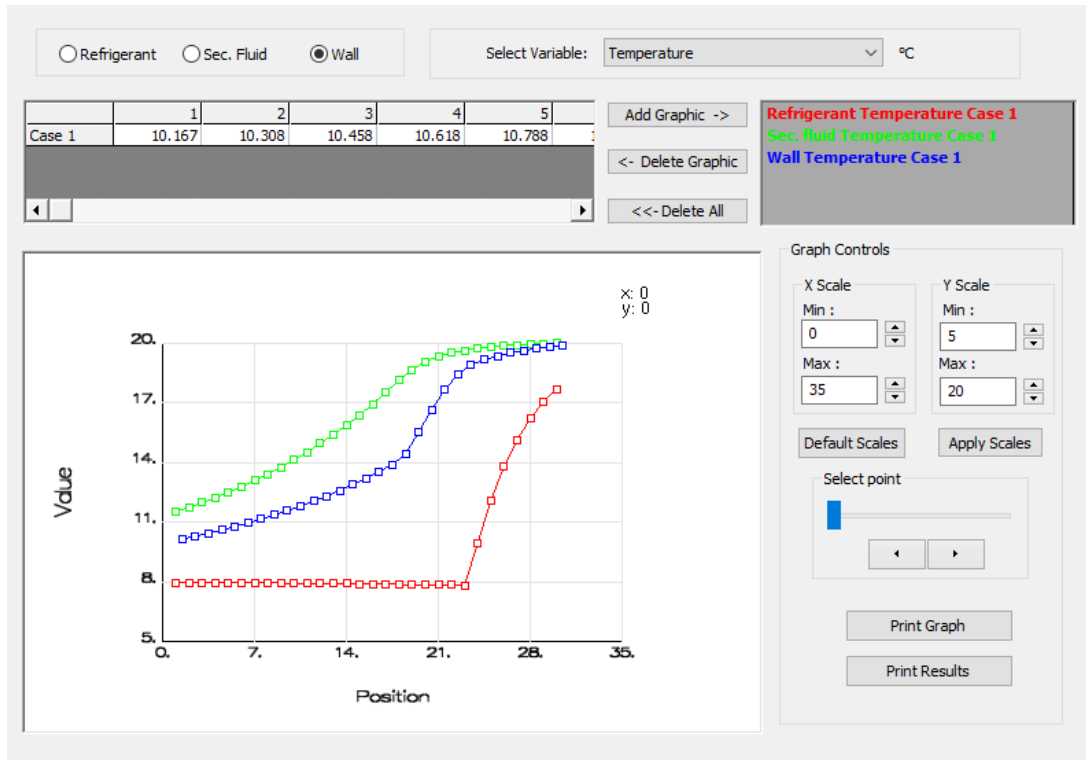
Figure 42. Temperature profile of the subexchanger 2.
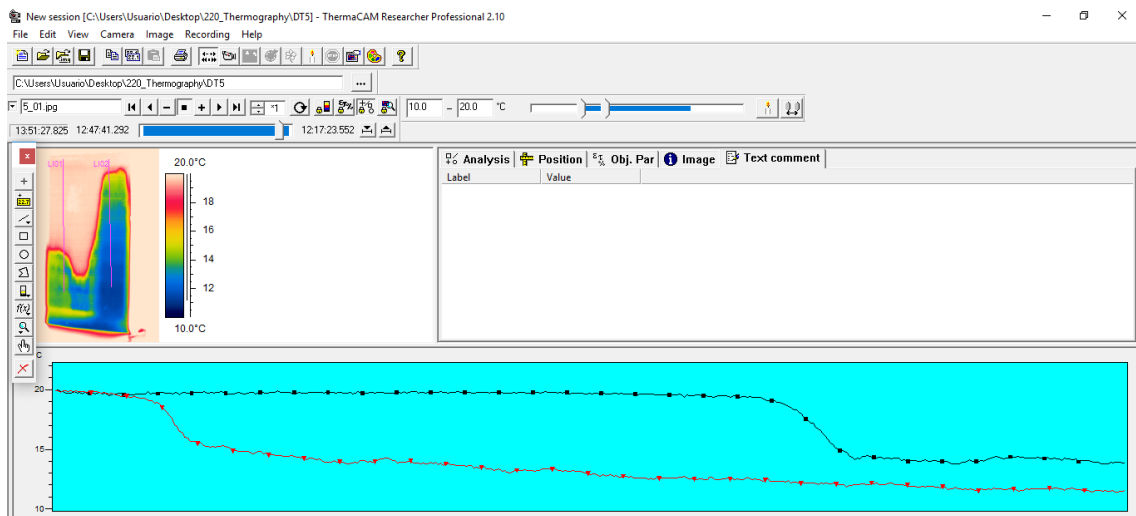
Figure 43. ThermoCam temperature profile from the thermography.

5.4 EVAPORATOR SIZE EVALUATION

A clear tendency of manufactures is the oversize of equipment due to economic and performance guarantee reasons. A bigger component is more expensive and ensures in the most cases a correct and the best working condition.

Thermography pictures point out a clear non-uniformity of temperature due to maldistribution. It suggests a possible oversize of the evaporator. It is stated by [43] and from a reasonable thinking that fluids do not distribute evenly through plates when the number of them are reasonable high.

Maldistribution is thought to change with geometry and size of the evaporator. As no experimental results are available for a smaller evaporator or/and with different plate number, a qualitative study has been performed. We used the tool IMST-ART that allows to simulate heat exchangers with high accuracy.

For a same working condition, a parametric study has been performed and represented in Figure 44. The evaporation temperature has been evaluated in function of the number of plates. Other important dimension as the length of the plates and port centres distances were not modified.
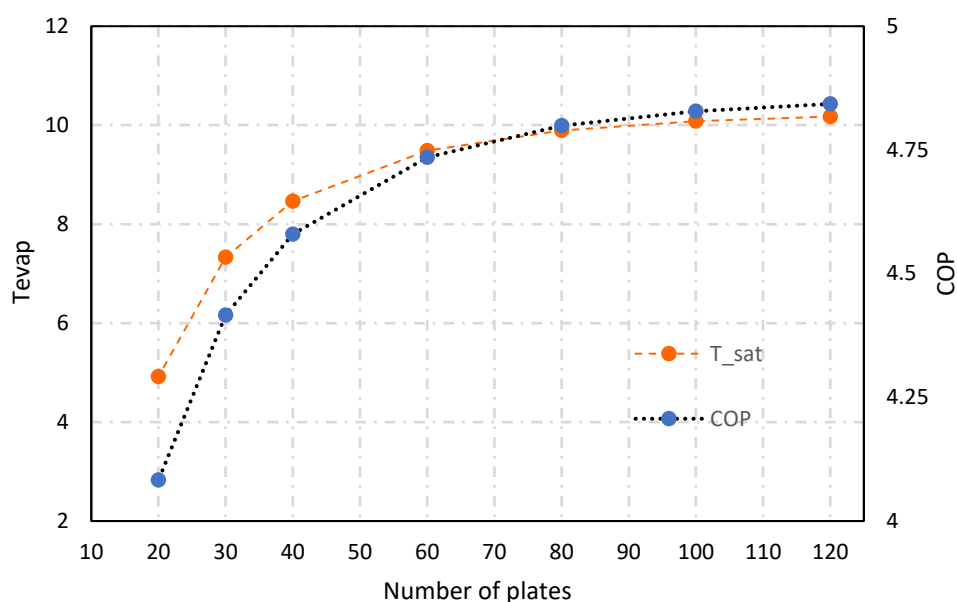
Figure 44. Evaporation and COP evolution for different sizes of evaporators. Operating conditions: SH=10 K and dTw=5 K

It is shown in Figure 44 how evaporation temperature changes with the number of plates. For a small HX, increasing the number of plates increases gradually evaporation temperature up to a given size, where the addition of more plates increases only slightly evaporation temperature. The addition of more plates just for guarantee reasons must be done cautiously as for a big evaporator almost no difference is observed, and the gained efficiency do not compensate the cost. Regarding the general performance of a system under the same working conditions, COP decrease like the observed with evaporation temperature. In the studied test-rig, the brazed plate heat exchanger under study has 120 plates and from this analysis is clearly stated its oversize.

It has been stated before, that for a given number of plates, the addition of plates does not increase the performance in a noticeable way. However, regarding the applied SH and water temperature drop, the decrease of evaporation temperature due to the decrease of the size of the evaporator is different.
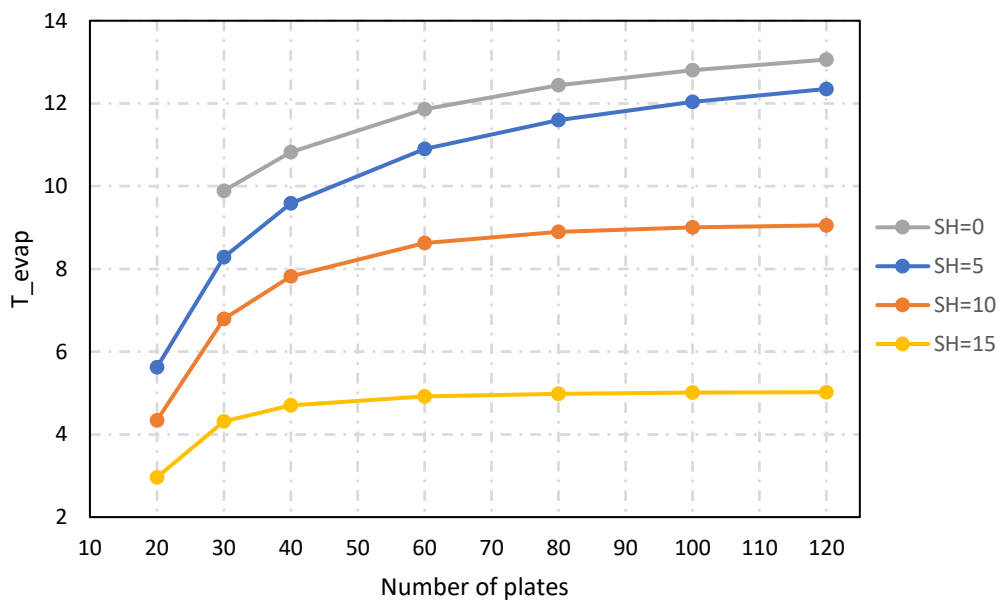
Figure 45. Evaporation temperature evolution with number of plates for dTw=5 K.
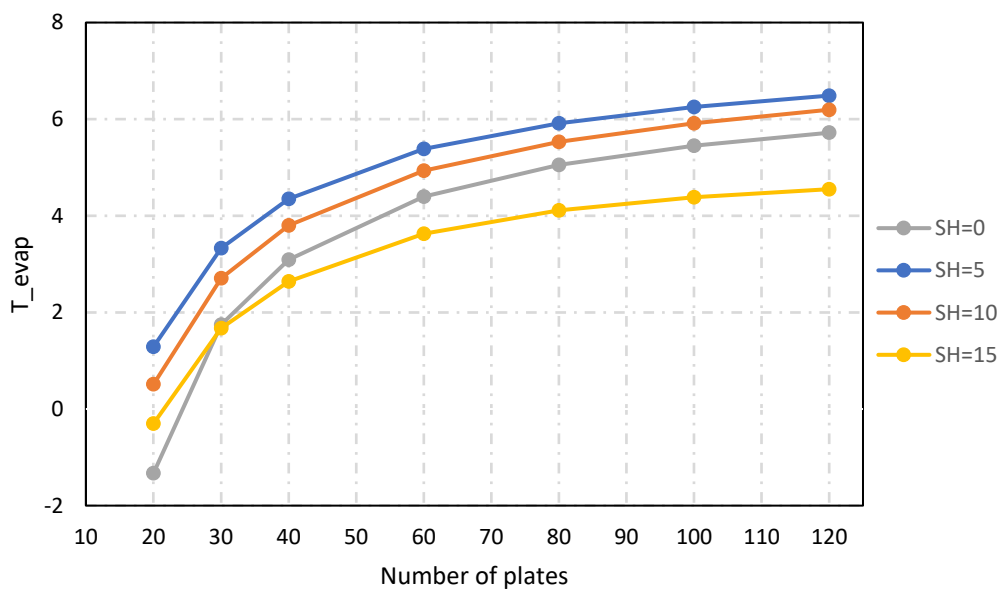
Figure 46. Evaporation temperature evolution with number of plates for dTw=13 K.

The experimental data has been introduced in IMST-ART and a similar analysis as before has been performed, to evaluate differences between SH. Shown in Figure 45, it can be observed that for dTw=5 and for low SH, the decrease of the size of the evaporator leads to a bigger drop than for higher SH. However, as shown in Figure 46 for dTw=13, this decrease is gradually and almost similar for each level of SH. For the test-rig, using the half of the actual number of plates would have led to a similar performance as evaporation temperature degradation due to the remove of plates is not noticeable

and leads to maximum a 2K decrease. However, the effect of maldistribution is not being taken into account.

It is from a point of view interesting to compare the evaporation temperature obtained from the experimental campaign with the evaporation drop suffered due to plate remove from a homogenous distribution evaluated with IMST-ART. In Table 9, the number of plates used that are comparable to the obtained evaporation temperature from the tests is shown. The obtained results are taken from the medium of the four tests made for each level of SH, this is for inlet quality x=0.07, 0.14, 0,2 and 0,3. It is observed that for dTw=5, a bigger percentage of the total area is used, corresponding a 36%, 50% and 31% to SH of 5, 10 and 15 respectively whereas for a dTw=13 the used percentage corresponds to an approximately 10% for the three degrees of SH. The cases for no SH almost no remarkable evaporation temperature difference is observed and a use of 100% of the total area of the evaporator is stated and observed in the taken thermographies.

From the point of view of the thermographies, the used area is bigger the lower the degree of SH. However, it can be thought that the bigger observed used area in the pictures corresponds with a lower evaporation temperature degradation, this is

Table 9. Degree of unused evaporator area.

dTw	SH	Number of plates	% of used Area	% of measured Area in thermography
	5	42	35	72
5	10	58	48	60
	15	48	40	40
	5	16	13	56
13	10	14	12	52
	15	18	15	50

In the next figures the influence of the size is observed for different water temperature drop in the evaporation temperature. It will be evaluated for high degree of superheat, 10 K and zero superheat as shown in Figure 47 and Figure 48 respectively. The water temperature inlet is 20ºC.

For high superheat and a small water temperature drop, the maximum possible evaporation temperature is achieved, the difference between the water temperature inlet and the level of superheat as stated in (1). In this case, the influence of the size of the area is not important as low area of the evaporator is needed. As the water temperature drop becomes higher, a bigger evaporator is needed to maintain the maximum possible evaporation temperature.

The case for low degree of superheat is different. The maximum possible evaporation temperature will be the difference of the inlet water temperature and the water temperature drop. However, the bigger the evaporator the closer to the maximum evaporation temperature.
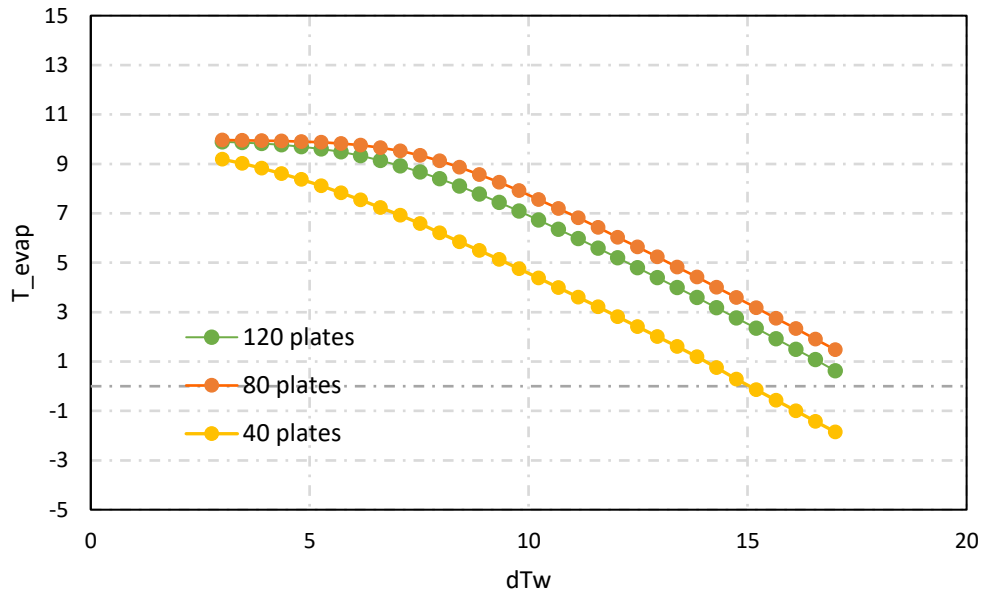
Figure 47. Evaporation temperature evaluation for different dTw and number of plates. SH=10 K
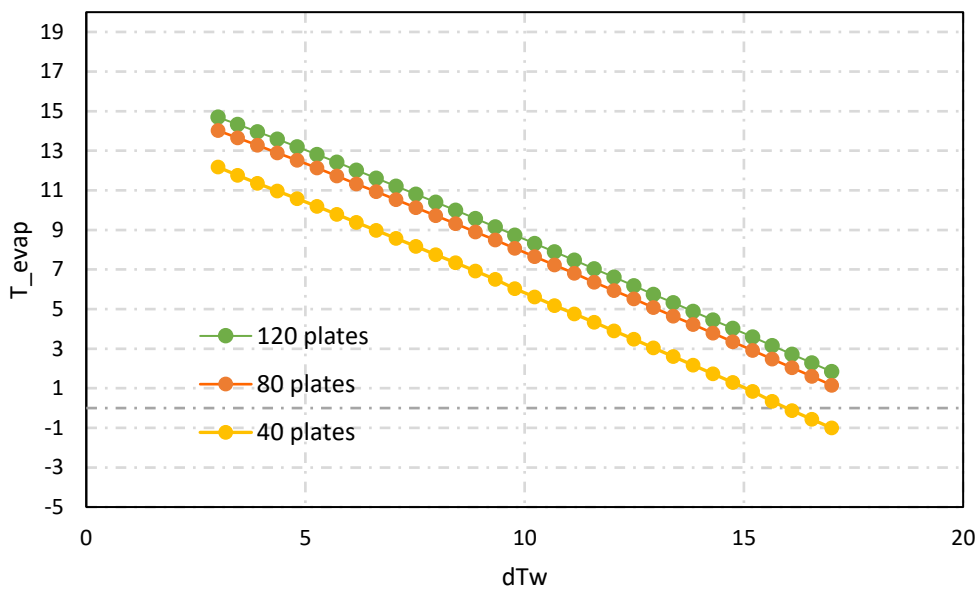
Figure 48. Evaporation temperature evaluation for different dTw and number of plates. SH=0K

The differences between working with superheat or not are now clear: the bigger size of the evaporator has great importance on the evaporation temperature when the superheat is higher than

the secondary temperature drop. As soon as the water temperature drop increases, the evaporation temperature drops, and the decrease becomes higher as smaller the evaporator is. This situation is similar to the experienced when the superheat is small, and the evaporator size should be big to avoid the evaporation temperature drop.

So, why is maldistribution causing a higher performance drop under certain working conditions observed during the test campaign? Here we take profit of the two-evaporator model to explain what is occurring but the assumption of a very high degree of maldistribution is made. Considering the evaporator big enough to separate it in two subexchangers, on the one hand in the first evaporator lower refrigerant is flowing through and high degree of superheat is registered at the outlet of the evaporator. On the other hand, higher mass flow is present in the second evaporator and lower superheat is measured. A scheme of the observed refrigerant maldistribution is represented in Figure 49.
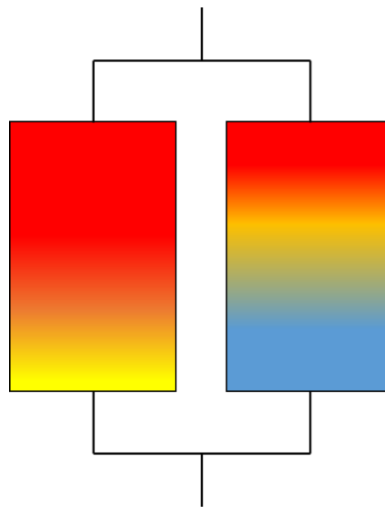
Figure 49. Schematic visualization of maldistribution in the two-evaporator model. The first evaporator has a bigger superheat than in the other.

It will be explained for the different working conditions how the evaporator will be working:

- SH>DT

The superheat is higher than the water temperature drop. As stated, the evaporation temperature will be the maximum possible to accommodate the degree of SH. As we have now a smaller evaporator than the original one, having a smaller evaporator has little effect on the performance of the evaporator, leading to no evaporation temperature drop. However, in the evaporator with almost no superheat, evaporation temperature must be adjusted as both must have the same. Therefore, in these cases the measured evaporation temperature in the test campaign agrees with the results with IMST-ART.

Although maldistribution is occurring, superheat will set the evaporation temperature and no degradation due to the uneven distribution of refrigerant is happening.

- DT=SH, DT>SH (SH≠0)

The water temperature drop is higher or equal to the superheat. As before explained, when having a high water temperature drop the decrease due to having a smaller evaporator becomes significant. Following the assumption of two subexchanger, the evaporator of the higher superheat suffers a bigger degradation the smaller this subexchanger is. The size of this subexchanger depends on the degree of maldistribution that exists. The evaporator with zero superheat decreases its evaporation temperature equal to the first subexchanger.

Maldistribution is in this case is degrading the performance of the evaporator as uneven superheat is occurring throughout the evaporator. Bigger differences between the expected results from IMST-ART and the experimental results are obtained.

- SH=0

This case is the superheat is fixed to zero, so both subexchanger have almost no level of superheat. Although maldistribution is occurring, the degradation is negligible. The evaporation temperature will be close to the maximum possible as bigger the evaporator is. Results with IMST-ART fit with the experimental results.

From this analysis, maldistribution has a bigger effect when a higher water temperature drop is applied in the application decreasing evaporation temperature drastically.

As performance degradation due to maldistribution cannot be quantified easily, maldistribution is simulated as a decrease in the U-value by authors [49]. The effect of maldistribution influences the total evaporator U-value due to uneven zones of superheat.
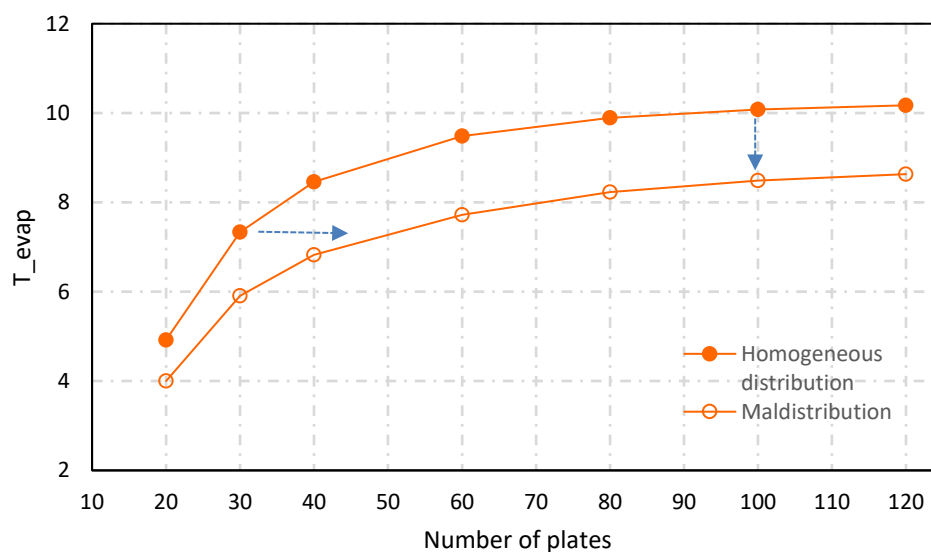
Figure 50. Counteract of maldistribution with the utilization of a bigger evaporator. Maldistribution cannot be reduced with a size increase when using a big evaporator.

Therefore, maldistribution can be counteracted by an increase of the heat exchanger size for small heat exchangers as shown in Figure 50. Maldistribution degradation occurring in larger heat exchangers cannot be recovered by size increase. It has been seen that having a bigger or smaller size has more or less influence depending on the application: for high water temperature glides, having a

bigger evaporator ensures a good performance. However, maldistribution effect should be considered in the design stage of the development of heat pumps and other similar projects as it causes the decrease of evaporation temperature leading to a general degradation of the system performance.
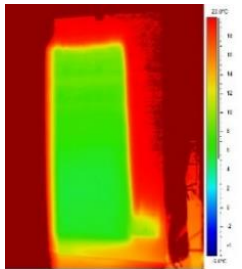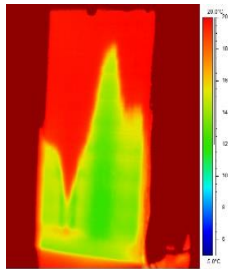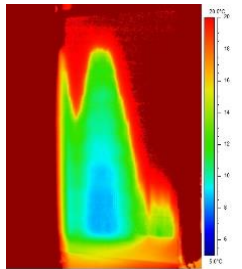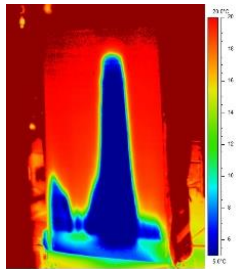
5.6 LOW INLET QUALITY INFLUENCE

Once the refrigerant leaves the expansion valve and entering the evaporator, the refrigerant consists of a mixture of vapor and liquid. For a given mass flux (refrigerant velocity) and quality, a flow pattern can be visualized. This has been commented in the literature review. For more information please refer to this part of the thesis.

Some test out of the main experimental matrix have been performed. It was expected a better distribution of the refrigerant when partly only liquid (small inlet qualities) was entering the evaporator. Flooded evaporators have only liquid at its entry and is suggested by manufactures as a solution for maldistribution. It has been observed that in the most part of the performed tests, refrigerant tends to accumulate at the furthest away from the inlet pipe of the evaporator.

Refrigerant mass flux depends on water flux (heat flux) within the test, but inlet quality can be changed and set to the desired value. In order to study the impact of inlet quality in the temperature distribution captured with IR, four examples are exposed in Table 10 with different water temperature glides and degrees of SH. Inlet qualities range from 0,015-0,06.

Table 10. Low inlet quality IR thermographies

a)	b)	c)	d)
T_{evap}= 4.05 ºC dTw= 12.9 x=0.042 SH=0	T_{evap}= 9.00 ºC dTw= 5 x=0.06 SH=10	T_{evap}= 5.89 ºC dTw= 9 x=0.015 SH=10	T_{evap}= -1.8 ºC dTw= 13 x=0.04 SH=10

It can be seen in Table 10, that for the lowest values of quality (a,b) a redistribution of refrigerant occurs towards the plates closer to the inlet. More common refrigerant distribution at the furthest

part of the inlet is observed as well (c). However, a central accumulation is occurring for the last example (d).

A general better distribution is observed for the case (a) without SH although part of the evaporator is not used. However, for (b,c) where 10 K SH is applied, temperature distribution suggest a better distribution. A worst case is observed in (d) where a central part of the evaporator is used.

Similar observation by [40] was observed by varying cooling capacity by means of increasing or decreasing compressor speed. However, no mention to the inlet quality was done. It is stated that mass flux is directly related to heat flux, so flow pattern is being changed within the compressor speed variation.
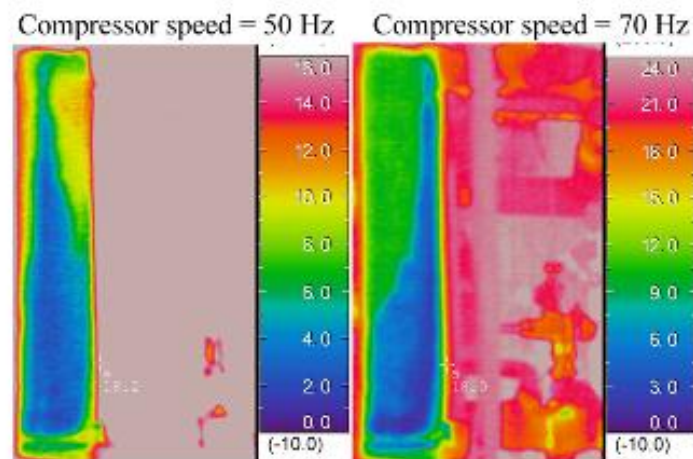
Figure 51. Temperature distributions indicating refrigerant distribution. Different accumulations can be observed by fixed SH=7.5 K [40]

From the own observations and others, it can be stated that flow pattern has a direct effect on refrigerant distribution. Low mass flow and low inlet quality, as stated by [23, 22], stratifies and liquid phase will enter the first channels. The formation of a liquid jet due to liquid momentum decides which plates will be overfilled. The quantity of vapor is in these cases small. More details and flow visualizations are out of scope of this project.

CHAPTER 6. CONCLUSIONS

6.1 GENERAL CONCLUSIONS

The main objective of this Master Thesis is the study of the refrigerant distribution in a brazed plate heat exchanger which is part of a water-to-water heat pump booster for DHW applications from European Project NXTGHP. To fulfill the target, maldistribution has been observed with thermography within different working conditions. General system performance for each working condition have been compared with simulation software which do not consider system degradation due to refrigerant maldistribution.

This problem is especially important in the evaporator as the refrigerant enters in it in two phase flow and usually the distribution of liquid and vapor is not uniform over all the channels. Well known in the literature, manufacturers have implemented some technical solutions like introducing distributors in the inlet port in order to minimize this effect. Nevertheless, the applied solutions usually are developed only for the nominal conditions and when the BPHE work in other conditions is difficult to know which is going to be its behavior.

When maldistribution occurs, evaporator surface temperature is distributed unevenly and can be registered with thermography as it is non-intrusive and non-contacting, having no influence in the evaporator. Inlet quality and superheat has been changed during the tests for a given water temperature difference to observe this phenomenon. Evaporation temperature has been registered for each case and compared with IMST-ART software results.

From the performed test campaign and its corresponding analysis following points can be stated:

- Maldistribution of refrigerant is observable with thermography and validated by measurements.
- Thermography pictures show a decrease of the available area used in the evaporator as refrigerant concentrates in a specific part of the heat exchanger.
- In Thermography pictures a clear tendency of the refrigerant to accumulate in the right part of the evaporator, the furthest part from the inlet. This tendency changes for low inlet qualities being this accumulation in the left part or in the centre. Refrigerant flow pattern changes may be the cause.
- Maldistribution has inherited a negative effect on evaporation temperature causing capacity and COP degradation. The decrease becomes more pronounced when high temperature glides at the water side are applied. Differences with simulation tool range from 2-9K.
- For nearly zero superheat working conditions, thermography pictures indicate in the most part of the cases full use of the area of the heat exchanger and a homogenous distribution of temperature is observed. However, refrigerant maldistribution cannot be exempted. Prediction with heat exchanger simulation tool is good and differ maximum 2K.

- Inlet quality at low superheat influences on evaporation temperature caused by maldistribution. At average inlet quality (x=0.14) lowest values are obtained.
- From a two-evaporator model assumption, maldistribution can be explained as a smaller use of the evaporator area and will affect more when working with a water temperature drop is higher than the applied SH. It is assumed that an oversized heat exchanger causes more uneven distribution of refrigerant. The COP degradation because of the refrigerant maldistribution is quite important for the performed test when working with higher water temperature drop than the degree of superheat. It is from this work stated that less evaporation temperature degradation occurs when the superheat is higher than the water temperature or equal to zero.

6.2 FUTURE WORK

This thesis encourages to continue working in the study of maldistribution: it is a nowadays issue and a possible handicap in the increase in sales of commercial heat pumps.

Systems to avoid maldistribution is leading by manufactures but other type of studied can be performed:

- Maldistribution in heat pumps with inverter compressor: how refrigerant is being distributed through plates when cooling capacity is being modulate
- Maldistribution in different evaporators: evaluate refrigerant distribution in different evaporator size, distributors, plate length…

CHAPTER 7. BUDGET

This chapter has the main objective of the breakdown of the expenses of the R&D (I+D in Spanish) activity performed within this Master Thesis. The duration of the project is 11 months. The project team is formed by project responsible, researcher expert and a junior researcher. Computer and thermographic camera are the main equipment used in the project. Fungible material is considered insignificant. The budget has been performed according to [51]. The budget includes therefore the following expenses:

- Manpower costs
- Inventorial material costs
- Fungible costs

7.1 MANPOWER COSTS

The budget of the staff dedicated to the project is the presented in the following tables. The costs associated to the junior researcher is evaluated apart from the professionals.

The costs due to overheads, social welfare and compensations are already included in the cost/hours values for professionals as stated in [51].

Table 11. Costs of professionals involved in this work

Professional Position	Cost/Hour (€/h)	Hours (h)	Costs
Project Responsible	51.4	30	1,542.00 €
Researcher Expert	39	50	1,950.00 €
TOTAL	**-**	**-**	**3,492.00 €**

The breakdown of the salary associated to the junior researcher is stated in the next table. The salary corresponds to a complete year. Overheads are already included:

Table 12. Costs associated to the junior researcher

Junior Researcher	Costs
Gross Annual Salary	21,404.88 €
Social Welfare (32.10%)	6,870.97€
Compensations (3.04%)	650.71 €
Travel and daily subsistence	-
TOTAL	**28,926.56 €**

Finally, the manpower total costs are summarized in the following table:

Table 13. Total Manpower costs

Manpower costs	Total Costs
Project Responsible	1,542.00 €
Researcher Expert	1,950.00 €
Junior Researcher	28,926.56 €
TOTAL	**32,418.56 €**

7.2 INVENTORIAL MATERIAL COSTS

In this section all the material used in this R&D activity is included.

the computer used by the junior researcher and its respective software for data and modelling issues and the thermographic camera for maldistribution observation within the performed tests are the main equipment.

The amortization of the following equipment is stated following the guidebook [51]:

Table 14. Equipment costs

Material	Usage (months)	Amortization period (years)	Costs	Percentage of use (%)	Amortization
Computer	11	6	585.00 €	60	53.63 €
Thermographic camera	11	10	30,000.00 €	40	600.00 €
TOTAL	-	-	-	**100**	**653.63 €**

The software used to perform this work has to be also considered. The software used and the associated costs are presented next. The percentage of use corresponds in total to the usage of the computer.

Table 15. Computer software costs

Software	Usage (months)	Amortization period (years)	Costs	Percentage of use (%)	Amortization
IMST-ART	11	6	1,200 €	20	36.66 €
Thermocam Pro	11	6	295.00 €	5	2.25 €
Microsoft Office	11	6	279.00 €	35	14.92 €
TOTAL	-	-	-	**60**	**53.83 €**

7.3 FUNGIBLE MATERIAL

Within this project, the office materials used will be considered within the overheads, because it is difficult to calculate the exact amount. The cost associated to fungible material can be considered low and rather insignificant and will be covered by the overheads considered in the total calculation of the budget.

7.4 TOTAL BUDGET

Table 16. Total costs

Total costs	Total Costs (€)
Manpower costs	32,418.56 €
Inventorial Material costs	707.46 €
Overheads (25%)	8,089.75 €
TOTAL	**41,215.77 €**

The total cost of this work amounts to forty-one thousand two hundred and fifteen euros and seventy-seven cents.

CHAPTER 8. REFERENCES

[1]   "Energy_consumption_in_households @ ec.europa.eu." .

[2]   "Index @ Yearbook.Enerdata.Net." .

[3]   F. Meggers and H. Leibundgut, "The potential of wastewater heat and exergy: Decentralized high-temperature recovery with a heat pump," *Energy Build.*, vol. 43, no. 4, pp. 879–886, Apr. 2011.

[4]   C. Arpagaus and S. Bertsch, "Task 4 Overview on R&D Switzerland, IEA HPT Annex 46 Domestic Hot Water Heat Pump, October 6, 2017," pp. 1–40, 2017.

[5]   E. C. Institute, "Heat Pumps: Integrating technologies to decarbonise heating and cooling," 2018.

[6]   S. S. Cipolla and M. Maglionico, "Heat recovery from urban wastewater: Analysis of the variability of flow rate and temperature in the sewer of Bologna, Italy," *Energy Procedia*, vol. 45, pp. 288–297, 2014.

[7]   R. Law, A. Harvey, and D. Reay, "Opportunities for low-grade heat recovery in the UK food processing industry," *Appl. Therm. Eng.*, vol. 53, no. 2, pp. 188–196, May 2013.

[8]   G. P. Panayiotou *et al.*, "Preliminary assessment of waste heat potential in major European industries," *Energy Procedia*, vol. 123, pp. 335–345, Sep. 2017.

[9]   F. Schmid, "Sewage Water: Interesting Heat Source for Heat Pumps and Chillers," *Conf. Proc. from 9th Int. IEA Heat Pump Conf. 20 – 22 May 2008, Zürich, Switz.*, no. May, p. 12, 2008.

[10]   A. Hepbasli, E. Biyik, O. Ekren, H. Gunerhan, and M. Araz, "A key review of wastewater source heat pump (WWSHP) systems," *Energy Convers. Manag.*, vol. 88, pp. 700–722, Dec. 2014.

[11]   G. Lorentzen and J. Pettersen, "A new, efficient and environmentally benign system for car air-conditioning," *Int. J. Refrig.*, vol. 16, no. 1, pp. 4–12, Jan. 1993.

[12]   G. Lorentzen, "Revival of carbon dioxide as a refrigerant," *Int. J. Refrig.*, vol. 17, no. 5, pp. 292–301, Jan. 1994.

[13]   P. Nekså, H. Rekstad, G. R. Zakeri, and P. A. Schiefloe, "CO2-heat pump water heater: characteristics, system design and experimental results," *Int. J. Refrig.*, vol. 21, no. 3, pp. 172–179, May 1998.

[14]   P. Nekså, "CO2 heat pump systems," *Int. J. Refrig.*, vol. 25, no. 4, pp. 421–427, Jun. 2002.

[15]   L. Cecchinato, M. Corradi, E. Fornasieri, and L. Zamboni, "Carbon dioxide as refrigerant for tap water heat pumps: A comparison with the traditional solution," *Int. J. Refrig.*, vol. 28, no. 8, pp. 1250–1258, Dec. 2005.

[16]   L. Cecchinato, M. Corradi, and S. Minetto, "Energy performance of supermarket refrigeration and air conditioning integrated systems," *Appl. Therm. Eng.*, vol. 30, no. 14–15, pp. 1946–1958, Oct. 2010.

[17]   "Quantum   Titan   340l."   [Online].   Available: https://www.solarhotwaterrepairsqld.com.au/systems/quantum-titan-340l.

[18]   M. Pitarch, E. Navarro-Peris, J. Gonzálvez-Maciá, and J. M. Corberán, "Evaluation of different heat pump systems for sanitary hot water production using natural refrigerants," *Appl. Energy*, vol. 190, pp. 911–919, Mar. 2017.

[19]   A. Redón, E. Navarro-Peris, M. Pitarch, J. Gonzálvez-Macia, and J. M. Corberán, "Analysis and optimization of subcritical two-stage vapor injection heat pump systems," *Appl. Energy*, vol. 124, pp. 231–240, Jul. 2014.

[20]   J. B. Jensen and S. Skogestad, "Optimal operation of simple refrigeration cycles: Part I: Degrees of freedom and optimality of sub-cooling," *Comput. Chem. Eng.*, vol. 31, no. 5–6, pp. 712–721, May 2007.

[21]   J. P. Koeln and A. G. Alleyne, "Optimal subcooling in vapor compression systems via extremum seeking control: Theory and experiments," *Int. J. Refrig.*, vol. 43, pp. 14–25, Jul. 2014.

[22]   J. M. Corberan and C. Montagud, "Project NxtHPG: next generation of heat pumps working with natural fluids," in *11th IIR Gustav Lorentzen Conference on Natural Refrigerants, Hangzhou, China. Conference Proceedings: ID 79*, 2014.

[23]   M. Pitarch, E. Navarro-Peris, J. Gonzálvez-Maciá, and J. M. Corberán, "Étude expérimentale portant sur un booster de pompe à chaleur en cycle souscritique destiné à la production d'eau chaude sanitaire et utilisant un sous-refroidisseur afin d'accroître l'efficacité du système à l'aide d'un frigorigène naturel (R290)," *Int. J. Refrig.*, vol. 73, pp. 226–234, Jan. 2017.

[24]   E. Hervas-Blasco, M. Pitarch, E. Navarro-Peris, and J. M. Corberán, "Study of different subcooling control strategies in order to enhance the performance of a heat pump," *Int. J. Refrig.*, vol. 88, pp. 324–336, Apr. 2018.

[25]   M. Pitarch, E. Hervas-Blasco, E. Navarro-Peris, J. Gonzálvez-Maciá, and J. M. Corberán, "Evaluation of optimal subcooling in subcritical heat pump systems," *Int. J. Refrig.*, vol. 78, pp. 18–31, Jun. 2017.

[26]   M. Pitarch, E. Navarro-Peris, J. Gonzálvez-Maciá, C. Montagud, and J. M. Corberan, "Influence of water lift temperature in transcritical and subcritical refrigerants," in *VII Congreso Ibérico de Ciencias y Técnicas del Fr{\'\i}o*, 2014.

[27]   G. A. Longo, "HC-290 (Propane) Vaporisation Inside a Brazed Plate Heat Exchanger," *Int. Refrig. Air Cond. Conf.*, vol. 1009, 2010.

[28]   G. A. Longo and A. Gasparella, "Heat transfer and pressure drop during HFC refrigerant vaporisation inside a brazed plate heat exchanger," *Int. J. Heat Mass Transf.*, vol. 50, no. 25–26, pp. 5194–5203, Dec. 2007.

[29]   S. Elbel and P. Hrnjak, "Flash gas bypass for improving the performance of transcritical R744 systems that use microchannel evaporators," *Int. J. Refrig.*, vol. 27, no. 7, pp. 724–735, Nov. 2004.

[30]   C. D. Bowers, S. S. Wujek, and P. Hrnjak, "Quantification of Refrigerant Distribution and Effectiveness in Microchannel Heat Exchangers Using Infrared Thermography," *Refrig. Air Cond.*, no. 2006, pp. 1–8, 2010.

[31]   C. D. Bowers, H. Mai, S. Elbel, and P. S. Hrnjak, "Refrigerant Distribution Effects on the Performance of Microchannel Evaporators," *Int. Refrig. Air Cond. Conf.*, pp. 1–11, 2012.

[32]   S. Vist, "Two-phase flow distribution in compact heat exchanger manifolds," *Exp. Therm. Fluid*

Sci., vol. 28, no. 2–3, p. 335, 2003.

[33]   C. D. Bowers and P. S. . Hrnjak, "Developing Two-Phase R134a Flow after an Expansion Valve in an 8 . 7mm Tube," *Int. Refrig. Air Cond.*, p. 11, 2008.

[34]   M. Ahmad, G. Berthoud, and P. Mercier, "General characteristics of two-phase flow distribution in a compact heat exchanger," *Int. J. Heat Mass Transf.*, vol. 52, no. 1–2, pp. 442–450, Jan. 2009.

[35]   M. Ahmad, G. Berthoud, and P. Mercier, "General characteristics of two-phase flow distribution in a compact heat exchanger," *Int. J. Heat Mass Transf.*, vol. 52, no. 1–2, pp. 442–450, Jan. 2009.

[36]   "SWEP Refrigerant Handbook: 6.6 SWEP distribution system." [Online]. Available: https://www.swep.net/refrigerant-handbook/6.-evaporators/asas5/.

[37]   M. K. Bassiouny and H. Martin, "Flow distribution and pressure drop in plate heat exchangers—I U-type arrangement," *Chem. Eng. Sci.*, vol. 39, no. 4, pp. 693–700, Jan. 1984.

[38]   M. K. Bassiouny and H. Martin, "Flow distribution and pressure drop in plate heat exchangers—II Z-type arrangement," *Chem. Eng. Sci.*, vol. 39, no. 4, pp. 701–704, Jan. 1984.

[39]   B. Thonon and P. Mercier, "Les échangeurs à plaques: dix ans de recherche au GRETh: Partie 2. Dimensionnement et mauvaise distribution," *Rev. Générale Therm.*, vol. 35, no. 416, pp. 561–568, Sep. 1996.

[40]   J. Claesson, "Doctoral Thesis. Thermal and Hydraulic Performance of Compact Brazed Plate Heat Exchangers Operating as Evaporators in Domestic Heat Pumps. KTH Energy Technology. ISBN: 91-7283-931-7," 2004.

[41]   J. K. Jensen, M. R. Kærn, T. Ommen, W. B. Markussen, L. Reinholdt, and B. Elmegaard, "Effect of liquid/vapour maldistribution on the performance of plate heat exchanger evaporators," in *Refrigeration Science and Technology*, 2015, pp. 2007–2014.

[42]   W. Brix, M. R. Kærn, and B. Elmegaard, "Modelling refrigerant distribution in microchannel evaporators," *Int. J. Refrig.*, vol. 32, no. 7, pp. 1736–1743, Nov. 2009.

[43]   W. Li and P. Hrnjak, "An experimentally validated model of single-phase flow distribution in brazed plate heat exchanger," *17th Int. Refrig. Air Cond. Conf. Purdue*, 2018.

[44]   M. R. Kærn, W. Brix, B. Elmegaard, and L. F. S. Larsen, "Compensation of flow maldistribution in fin-and-tube evaporators for residential air-conditioning," *Int. J. Refrig.*, vol. 34, no. 5, pp. 1230–1237, 2011.

[45]   SWEP, "SWEP distribution system," *SWEP Refrigerant handbook*. [Online]. Available: https://www.swep.net/refrigerant-handbook/6.-evaporators/asas5/. [Accessed: 17-Jan-2019].

[46]   A. S. Danfoss, "Most valves expand your refrigerant, EcoFlow™ expands your options."

[47]   M. Pitarch, E. Navarro-Peris, J. Gonzálvez-Maciá, and J. M. Corberán, "Experimental study of a subcritical heat pump booster for sanitary hot water production using a subcooler in order to enhance the efficiency of the system with a natural refrigerant (R290)," *Int. J. Refrig.*, vol. 73, pp. 226–234, Jan. 2017.

[48]   J. M. Corberan *et al.*, "'ART' A Computer Code To Assist The Design Of Refrigeration and A/C Equipment," *Int. Refrig. Air Cond. Conf.*, no. 34, pp. 1–8, 2002.

[49]   G. Mader, *Economic analysis of air-water heat pump technologies with a screening method*. 2015.

[50]   P. Fei and P. S. Hrnjak, "Adiabatic Developing Two-Phase Refrigerant Flow in Manifolds of Heat

Exchangers," *Air Cond. Refrig. Center, Univ. Illinois*, vol. 61801, no. 217, 2004.

[51]   UPV, "RECOMENDACIONES EN LA ELABORACIÓN DE PRESUPUESTOS EN ACTIVIDADES DE I+D+I (REVISIÓN 2018)," 2018.